



NRL/MR/6180--17-9728

## Quantification of Sulfur in Mobility Fuels

BRIAN T. FISHER

JEFFREY A. CRAMER

MARK H. HAMMOND

KATHERINE M. HINNANT

*Navy Technology Center for Safety and Survivability  
Chemistry Division*

ROBERT E. MORRIS

*Nova Research Inc.  
Alexandria, Virginia*

April 20, 2017

Approved for public release; distribution is unlimited.

REPORT DOCUMENTATION PAGE				Form Approved OMB No. 0704-0188	
Public reporting burden for this collection of information is estimated to average 1 hour per response, including the time for reviewing instructions, searching existing data sources, gathering and maintaining the data needed, and completing and reviewing this collection of information. Send comments regarding this burden estimate or any other aspect of this collection of information, including suggestions for reducing this burden to Department of Defense, Washington Headquarters Services, Directorate for Information Operations and Reports (0704-0188), 1215 Jefferson Davis Highway, Suite 1204, Arlington, VA 22202-4302. Respondents should be aware that notwithstanding any other provision of law, no person shall be subject to any penalty for failing to comply with a collection of information if it does not display a currently valid OMB control number. <b>PLEASE DO NOT RETURN YOUR FORM TO THE ABOVE ADDRESS.</b>					
1. REPORT DATE (DD-MM-YYYY) 20-04-2017		2. REPORT TYPE Memorandum Report		3. DATES COVERED (From - To) January 1, 2016 – December 31, 2016	
4. TITLE AND SUBTITLE  Quantification of Sulfur in Mobility Fuels				5a. CONTRACT NUMBER N0001416WX00239	
				5b. GRANT NUMBER	
				5c. PROGRAM ELEMENT NUMBER 0603640M	
6. AUTHOR(S)  Brian T. Fisher, Jeffrey A. Cramer, Mark H. Hammond, Katherine M. Hinnant, and Robert E. Morris*				5d. PROJECT NUMBER 2223	
				5e. TASK NUMBER	
				5f. WORK UNIT NUMBER 61-9496-06	
7. PERFORMING ORGANIZATION NAME(S) AND ADDRESS(ES)  Naval Research Laboratory 4555 Overlook Avenue, SW Washington, DC 20375-5320				8. PERFORMING ORGANIZATION REPORT NUMBER  NRL/MR/6180--17-9728	
9. SPONSORING / MONITORING AGENCY NAME(S) AND ADDRESS(ES) Office of Naval Research Attn: Mr. Billy Short One Liberty Center 875 N. Randolph St., Suite 1425 Arlington, Virginia 22203-1995				10. SPONSOR / MONITOR'S ACRONYM(S) ONR 6.3	
				11. SPONSOR / MONITOR'S REPORT NUMBER(S)	
12. DISTRIBUTION / AVAILABILITY STATEMENT  Approved for public release; distribution is unlimited.					
13. SUPPLEMENTARY NOTES  *Nova Research Inc., Alexandria, VA					
14. ABSTRACT  Methods to quantify sulfur in mobility fuels, particularly for concentrations below 10 ppm, were examined and evaluated at the Naval Research Laboratory (NRL). Work was divided into three primary thrusts: infrared (IR) spectroscopy for direct liquid-phase analysis, electrochemical SO <sub>2</sub> measurements, and optical SO <sub>2</sub> measurements. Much of the work focused on SO <sub>2</sub> as a single analyte that could be produced via lean combustion of liquid fuel. Results showed that IR spectroscopy does not have a sufficient, generalized sensitivity toward the range of sulfur compounds typically found in liquid fuels. Cermet (ceramic-metallic) sensor measurements showed promise in terms of response and sensitivity to SO <sub>2</sub> , but the sensor progressively degraded and became completely unresponsive. For combustion exhaust gas analysis, conventional NDIR (non-dispersive infrared) instruments do not have sufficient sensitivity to SO <sub>2</sub> , whereas UVF (ultraviolet fluorescence) instruments have the required sensitivity but suffer from performance issues related to other combustion products present (NO, CO, and unburned hydrocarbons). A commercial electrochemical SO <sub>2</sub> sensor showed promise, but might not have sufficient sensitivity and exhibited significant cross-sensitivity to other combustion products.					
15. SUBJECT TERMS Sulfur                      Mobility fuels                      Electrochemical sensors Sulfur dioxide           Infrared absorption           Ultraviolet Fluorescence SO <sub>2</sub> Cermet					
16. SECURITY CLASSIFICATION OF:			17. LIMITATION OF ABSTRACT  Unclassified Unlimited	18. NUMBER OF PAGES  44	19a. NAME OF RESPONSIBLE PERSON Brian T. Fisher
a. REPORT Unclassified Unlimited	b. ABSTRACT Unclassified Unlimited	c. THIS PAGE Unclassified Unlimited			19b. TELEPHONE NUMBER (include area code) (202) 404-3365



## CONTENTS

<b>INTRODUCTION.....</b>	<b>1</b>
<b>Review of Commercial Sensors .....</b>	<b>1</b>
<i>Species-independent Sulfur Detection.....</i>	<i>1</i>
<i>Sulfur Monoxide (SO) Detection .....</i>	<i>2</i>
<i>Sulfur Dioxide (SO<sub>2</sub>) Detection .....</i>	<i>3</i>
<i>Hydrogen Sulfide (H<sub>2</sub>S) Detection .....</i>	<i>3</i>
<i>Simultaneous Detection of Multiple Sulfur Species.....</i>	<i>3</i>
<i>Indirect Sulfur Detection.....</i>	<i>4</i>
<b>Mid-infrared and Near-infrared Spectroscopy for Measurement of Sulfur in Liquid-phase Fuel</b>	<b>4</b>
<b>Cermet Sensors and Cyclic Voltammetry .....</b>	<b>5</b>
<b>Optical Methods for Measurement of Sulfur in Combustion Exhaust Gas .....</b>	<b>5</b>
<b>Conversion of Sulfur to SO<sub>2</sub> via Combustion.....</b>	<b>5</b>
<b>OBJECTIVE .....</b>	<b>6</b>
<b>INFRARED SPECTROSCOPY FOR DIRECT LIQUID-PHASE ANALYSIS.....</b>	<b>6</b>
<b>Experimental Setup .....</b>	<b>6</b>
<i>Spectrophotometer .....</i>	<i>6</i>
<i>Data Processing and Preprocessing .....</i>	<i>7</i>
<b>Results and Discussion .....</b>	<b>7</b>
<i>Initial NIR/IR Organosulfur Compound Survey.....</i>	<i>7</i>
<i>Fuel Surrogates.....</i>	<i>10</i>
<i>Extreme Fuel Surrogate/Organosulfur Compound Blending.....</i>	<i>11</i>
<i>ATR NIR Multivariate Modeling .....</i>	<i>14</i>
<i>Quartz Cuvette NIR Multivariate Modeling.....</i>	<i>15</i>
<i>Assessment of Modeling IR Spectra .....</i>	<i>17</i>
<b>Conclusions .....</b>	<b>17</b>
<b>ELECTROCHEMICAL MEASUREMENTS OF SO<sub>2</sub> .....</b>	<b>18</b>
<b>Cermet Sensors .....</b>	<b>18</b>
<i>Experimental Setup .....</i>	<i>18</i>
<i>Results and Discussion.....</i>	<i>19</i>
<i>Conclusions .....</i>	<i>24</i>
<b>Commercial SO<sub>2</sub> Sensor .....</b>	<b>25</b>
<i>Experimental Setup .....</i>	<i>25</i>

<i>Results and Discussion</i> .....	25
<i>Conclusions</i> .....	28
<b>OPTICAL MEASUREMENTS OF SO<sub>2</sub></b> .....	<b>28</b>
<b>Experimental Combustor Setup</b> .....	<b>28</b>
<b>Initial Validation Experiments</b> .....	<b>29</b>
<b>Ultraviolet Fluorescence Measurements</b> .....	<b>31</b>
<b>Commercial Electrochemical Sensor Measurements</b> .....	<b>31</b>
<b>SUMMARY AND CONCLUSIONS</b> .....	<b>32</b>
<b>POTENTIAL FUTURE WORK</b> .....	<b>33</b>
<b>ACKNOWLEDGMENTS</b> .....	<b>33</b>
<b>REFERENCES</b> .....	<b>33</b>

## FIGURES

Fig. 1: Visual representation of vibrational mode frequency ranges for various sulfur-bearing compounds (from Ref. 37). .....	4
Fig. 2: Model organosulfur compounds examined in this study. ....	8
Fig. 3: Infrared absorbance spectrum of neat di-t-butyl disulfide, showing C-S, C-C and S-S stretching modes at about 800 $\text{cm}^{-1}$ and 550 $\text{cm}^{-1}$ , respectively. ....	8
Fig. 4: Infrared absorbance spectrum of neat 2-hexylthiophene, showing the C-S stretching mode at about 815 $\text{cm}^{-1}$ . ....	9
Fig. 5: Infrared absorbance spectrum of neat 3-methylbenzothiophene, showing the C-S stretching mode at about 835 $\text{cm}^{-1}$ . ....	9
Fig. 6: Infrared absorbance spectrum of neat 4,6-dimethyldibenzothiophene, showing two C-H out of plane bending modes at about 770 $\text{cm}^{-1}$ and 890 $\text{cm}^{-1}$ and the C-S stretching mode at about 825 $\text{cm}^{-1}$ . ....	10
Fig. 7: Full-spectrum absorbance of neat surrogate fuels obtained with the ATR accessory. ....	11
Fig. 8: Comparison of a sulfur-relevant range of absorbance results obtained from a pure organosulfur compound (small-dashed line), neat jet fuel surrogate (solid line), and a rough 50/50 blend of the two samples (long-dashed line). ....	12
Fig. 9: The comparison seen in Figure 8, with the 50/50 blend replaced with a more modest 5,000 ppm sulfur blend (long-dashed line). ....	12
Fig. 10: Comparison of a sulfur-relevant range of absorbance results obtained from a pure organosulfur compound (small-dashed line), neat jet fuel surrogate (solid line), and a 5,000 ppm blend of the two samples (long-dashed line), all obtained through the use of salt plates. ....	13
Fig. 11: Comparison of a sulfur-relevant range of absorbance results obtained from pure 1-pentanethiol compound (small-dashed line), neat jet fuel surrogate (solid line), and a 5,000 ppm blend of the organosulfur compound in the surrogate fuel (long-dashed line). ....	13
Fig. 12: NIR spectra acquired from the samples used to produce Table 3 using a 5-mm pathlength quartz cuvette. ....	16
Fig. 13: Schematic of experimental setup for cermet sensor testing. ....	19
Fig. 14: Cyclic voltammogram curves for each of the four elements of a working cermet sensor array when exposed to air. ....	19
Fig. 15: Background-subtracted, unfolded, and concatenated cermet signal showing difference between response to clean air (blue) and response to 5 ppm $\text{SO}_2$ (black). ....	20
Fig. 16: Principal component analysis (PCA) plot showing clear response in PC1 (first principal component) to 5 ppm $\text{SO}_2$ exposure, even in the presence of sensor drift. ....	20
Fig. 17: Sensor response for three consecutive exposures to 4 ppm $\text{SO}_2$ . Abscissa (x-axis) value is sample number, and each sample spans an entire 15-second voltage cycle. Ordinate (y-axis) value for each point is the sum of the sensor response (electrical current) over an entire 15-second voltage cycle. ....	21

Fig. 18: Sensor response to SO <sub>2</sub> for 0.2 ppm, 0.5 ppm, 1 ppm, 2 ppm, and 4 ppm concentrations in an increasing-decreasing-increasing pattern. Abscissa (x-axis) value is sample number, and each sample spans an entire 15-second voltage cycle. Ordinate (y-axis) value for each point is the sum of the sensor response (electrical current) over an entire 15-second voltage cycle.....	22
Fig. 19: Sensor response to SO <sub>2</sub> for 0.1 ppm, 0.25 ppm, 0.5 ppm, and 1 ppm concentrations, in ascending order. Abscissa (x-axis) value is sample number, and each sample spans an entire 15-second voltage cycle. Ordinate (y-axis) value for each point is the sum of the sensor response (electrical current) over an entire 15-second voltage cycle.....	22
Fig. 20: Sensor response to SO <sub>2</sub> for 0.1 ppm, 0.25 ppm, 0.5 ppm, 1 ppm, 2 ppm, and 4 ppm concentrations, in triplicate and in ascending order. Abscissa (x-axis) value is sample number, and each sample spans an entire 15-second voltage cycle. Ordinate (y-axis) value for each point is the sum of the sensor response (electrical current) over an entire 15-second voltage cycle. ....	23
Fig. 21: Raw cyclic voltammograms for baseline air-exposure measurements from the initial sensor survey (black trace) and from experiments relevant to Figure 20 (blue trace). ....	24
Fig. 22: Sensor response to SO <sub>2</sub> for 0.2 ppm, 0.5 ppm, 1 ppm, 2 ppm, and 4 ppm concentrations in an increasing-decreasing pattern. Abscissa (x-axis) value is sample number, and each sample spans an entire 15-second voltage cycle. Ordinate (y-axis) value for each point is the sum of the sensor response (electrical current) over an entire 15-second voltage cycle. ....	24
Fig. 23: Schematic of experimental setup for testing with Dräger SO <sub>2</sub> sensors. ....	25
Fig. 24: Observed SO <sub>2</sub> concentrations vs. actual SO <sub>2</sub> concentrations over a 3-week period. Short-dashed lines indicate linear regression fits to the experimental data. The long-dashed gray line illustrates a perfect match between observed and actual SO <sub>2</sub> concentrations. Error bars represent ± one standard deviation for the replicate measurements. ....	26
Fig. 25: Observed SO <sub>2</sub> concentrations in presence of humidified air containing ~4000 ppm CO <sub>2</sub> and ~400 ppm CO. Exposure to SO <sub>2</sub> was in a repeating pattern of 0.2 ppm, 0.5 ppm, 1 ppm, 2 ppm, and 4 ppm. ...	27
Fig. 26: Photograph of liquid-fuel combustor developed to measure SO <sub>2</sub> in combustion exhaust.....	28
Fig. 27: Photograph of individual components of liquid-fuel combustor.....	29
Fig. 28: Fuel sulfur concentration based on measured exhaust SO <sub>2</sub> concentration vs. known fuel sulfur concentration.....	30

## TABLES

Table 1: Summary of COTS instruments for sulfur species detection.....	2
Table 2: Expected SO <sub>2</sub> concentrations (by volume) in combustion exhaust, assuming 100 ppm (by weight) of the various sulfur compounds in either dodecane (C <sub>12</sub> H <sub>26</sub> ) or tetradecane (C <sub>14</sub> H <sub>30</sub> ) fuel. ....	6
Table 3: Results of modeling sulfur content of model organosulfur compounds in dodecane from 11,450–8,000 cm <sup>-1</sup> (874–1,250 nm) using PLS regression of spectra acquired with ATR. ....	15
Table 4: Results of modeling sulfur content of model organosulfur compounds in dodecane from 11,450–8,000 cm <sup>-1</sup> (874–1,250 nm) using PLS regression of spectra acquired from 5 mm quartz cuvettes. ....	16
Table 5: Results of modeling sulfur content of model organosulfur compounds in dodecane from 11,450–8,000 cm <sup>-1</sup> (874–1,250 nm) using PLS regression of spectra acquired from 5 mm quartz cuvettes, with 1 LV arbitrarily selected as the optimal number to use. ....	17
Table 6: Cross-sensitivity of DrägerSensor XXS SO <sub>2</sub> sensor to potential combustion exhaust gases. ....	26
Table 7: Summary of exposures and results of SO <sub>2</sub> and CO/CO <sub>2</sub> /NO testing for Units 167 / 168.....	27
Table 8: Measurement ranges of ZRE exhaust gas analyzer units for various gas species of interest. All values are volume/mole fractions. ....	29

# QUANTIFICATION OF SULFUR IN MOBILITY FUELS

## INTRODUCTION

Liquid hydrocarbon fuels can be reformed to generate hydrogen for fuel cells. Unfortunately, the non-negligible amounts of sulfur present in many of these fuels can poison and deactivate the catalysts typically used in fuel cells. Thus, there is a need for a method to detect and quantify sulfur content in mobility fuels that serve as feedstocks for fuel cell hydrogen reformers. Furthermore, it is preferred that the methods and instrumentation to be used can be implemented in a simple and safe in-line system between the liquid fuel storage container and the fuel reformer. There are several candidate methods for meeting these requirements, as described in this report.

Sulfur occurs naturally in petroleum and is limited to 0.3 wt % total sulfur in Jet A, JP-8, JP-5 and TS-1 jet fuels. F-76 diesel fuel is limited to a total sulfur content of 0.5 wt %, while marine gas oils (MGO) can contain as much as 1.0 wt % total sulfur. Currently, the industry is moving towards low-sulfur fuels with an interim sulfur limit of 500 ppm (0.05 wt %), which will ultimately be replaced by ultra-low sulfur diesel (ULSD) with a limit of 15 ppm (0.0015 wt %) sulfur. Most F-76 diesel fuel currently procured by the Navy is either low- or ultralow-sulfur.

Sulfur in petroleum-based fuels is most commonly present as thiols (mercaptans), disulfides, sulfides, thiophenes or benzothiophenes. The compositional diversity of organosulfur compounds thus requires either a detection method sensitive to all possible forms of sulfur or a method whereby all the various forms of sulfur are converted to one analyte. Both approaches were explored in this program.

## Review of Commercial Sensors

Table 1 summarizes a wide range of commercial-off-the-shelf (COTS) options for sulfur quantification. The various instruments are grouped according to the detected species, and described in terms of limit of detection (LOD) of the analyte, size, and cost. We assume that LOD and size are the two most important factors, in terms of feasibility for deployment of a field unit device for the detection and quantification of sulfur in mobility fuels. It is important to note that the limits of detection shown in Table 1 are approximate, and are specific to the particular analyte for each instrument. The exact relationship between the analyte (e.g., SO, SO<sub>2</sub>, etc.) and the total sulfur weight fraction in the original liquid fuel is unknown and likely depends on multiple factors. Given the program goal of an instrument or system with reasonably small size, reasonably low cost, and extremely high sensitivity, the most likely options among the COTS sensors seem to be those that measure sulfur dioxide (SO<sub>2</sub>). Some of the instruments shown in Table 1 are described below in more detail.

### *Species-independent Sulfur Detection*

Gas Chromatography-Atomic Emission Detection (GC-AED) can be used to detect sulfur [1], with a reported sulfur limit of detection (LOD) in the literature of about 1 ppm [2]. Agilent sells a commercial AED detector, but it would appear to be rather large for the purposes of the present work [3]. Inductively coupled plasma-optical emission spectrometry (ICP-OES), while an effective sulfur analysis technique for fuels [4] that also utilizes atomic emission principles, has the same drawback, judging by the commercial ICP-OES instruments sold by Spectro [5]. The use of laser induced breakdown spectroscopy (LIBS), another type of atomic emission spectroscopy, might also be considered, as at least Oxford Instruments produces handheld LIBS instrumentation [6], though it is unknown what the sulfur LOD would be for such an instrument.

Table 1: Summary of COTS instruments for sulfur species detection.

Instrument	Manufacturer	Technique	Size <sup>a</sup>	Cost <sup>b</sup>	Analyte LOD <sup>c</sup>
<b>Species-independent Sulfur Detection:</b>					
G2350A	Agilent	GC-AED	OOO	\$\$\$	1 ppm
Arcos	Spectro	ICP-OES	OOO	\$\$\$	<10 ppm
Genesis	Spectro	ICP-OES	OOO	\$\$\$	<10 ppm
MESA-7220	Horiba	XRF	OO	\$\$\$	<1 ppm
Sindie 2622	X-Ray Optical Systems	XRF	OO	\$\$\$	<1 ppm
Lab-X3500	Oxford Instruments	XRF	OO	\$\$\$	<1 ppm
<b>SO Detection:</b>					
8355 SCD	Agilent	chemiluminescence	OO	\$\$\$	<0.1 ppm
Antek 7090	PAC	chemiluminescence	OO	\$\$\$	<0.1 ppm
<b>SO<sub>2</sub> Detection:</b>					
PAC 7000	Dräger	electrochem. sensor	O	\$	1 ppm
6400T	Teledyne	UVF	OO	\$\$\$	<0.1 ppm
SOLA II Flare	ThermoFisher	UVF	OOO <sup>d</sup>	\$\$\$ <sup>d</sup>	<0.1 ppm
<b>H<sub>2</sub>S Detection:</b>					
PAC 5500	Dräger	electrochem. sensor	O	\$	0.1 ppm
HS-03	RKI	electrochem. sensor	O	\$	0.5 ppm
<b>Multiple-species Detection:</b>					
FPD	Buck Scientific	flame photometry	OO	\$\$	0.2 ppm
FPD Plus	Agilent	flame photometry	OO	\$\$	<0.5 ppm
PFPD	OI Analytical	flame photometry	OO	\$\$	<2 ppm

<sup>a</sup> OOO = larger than small benchtop instrument; OO = small benchtop instrument; O = handheld

<sup>b</sup> \$\$\$ = >\$10,000; \$\$ = \$1,000 – \$10,000; \$ = <\$1,000

<sup>c</sup> limit of detection for analyte of interest for each instrument (e.g., SO, SO<sub>2</sub>, etc.)

<sup>d</sup> combustor is an integrated component of the instrument

Horiba sells the MESA-7220, a sulfur detector intended for use with fuels and oils, which has a reported LOD for sulfur, regardless of speciation, below 1 ppm [7]. This instrument provides an element-specific quantification via x-ray fluorescence (XRF), the technique upon which ASTM D7220 [8] is based. In addition, X-Ray Optical Systems sells the Sindie 2622 [9] and Oxford Instruments sells the Lab-X3500 [10], both instruments that look to be roughly similar to the MESA-7220 in terms of underlying technology, size, and sulfur LOD. Rigaku also sells multiple comparable XRF-based sulfur detection instruments as well [11]. Unfortunately, all of these instruments are benchtop units that do not appear to be quite small enough for the present work. In addition to size considerations, it must also be noted that the potential complications associated with the use of an apparatus capable of emitting high-energy X-rays in the context of fuel cell work should be considered.

#### *Sulfur Monoxide (SO) Detection*

The primary method for SO detection is chemiluminescence. The Agilent 8355 sulfur chemiluminescence detector (SCD) [12] operates by combusting sulfur-containing compounds into sulfur monoxide, which then photochemically reacts with ozone (produced by a generator within the instrument

itself) to produce a measurable signal. This detector meets the analysis standards set forth in ASTM D5623 [13], but only if it is interfaced with gas chromatography (GC) instrumentation [14]. Given that the detector does not appear to be a small unit [15] even before attaching a GC, it will most likely not suit the needs of the present work. Other instruments that meet ASTM D5623 standards, including the PAC Antek 7090 [16] (also an SCD instrument, also compliant with ASTM D5504-specific GC-chemiluminescence sulfur detection standards [17]) would appear to have similar size limitations.

### *Sulfur Dioxide (SO<sub>2</sub>) Detection*

Dräger sells a handheld gaseous sulfur dioxide detector (model 7000 [18]) with a reported SO<sub>2</sub> LOD of about 1 ppm [19]. This detector's use of an electrochemical sensor can be inferred from Dräger's own literature [20]. Despite this sensor's small size, implementing this sensing solution would still require the sulfur in the fuel analyte to be converted entirely to SO<sub>2</sub>, most likely, though not necessarily, through combustion. Two of these sensors were acquired and used in this program to evaluate small, handheld COTS technologies.

Ultraviolet fluorescence (UVF) of SO<sub>2</sub> is the basis for a gas analyzer that we have acquired and used in this program. There are several issues that limit its capabilities in the context of our work, as described in a later section of this report, though it is at least conceivable that other UV fluorescence instruments might not possess identical drawbacks. Teledyne sells an integrated UVF instrument [21], meeting ASTM D5453 standards [22], with a reported limit of detection below 1 ppm. The instrument has a built-in conversion capability that utilizes either combustion or electrical heating to transform all sulfur compounds in the analyte into sulfur dioxide prior to measurement. The stand-alone detector itself (model 6400E [23]) is fairly small, but perhaps not quite small enough for actual use in the context of the present fuel cell work, especially considering the necessity of an additional combustor or similar conversion unit. It might be noted that larger UVF-based sulfur analysis instruments for petrochemical products are also available commercially [24], indicating the established utility of the technique. UVF would also appear to be the sulfur analysis technique already utilized by regulators in California for the purposes of ensuring that gasoline and diesel fuels comply with state sulfur specifications [25], and there is at least one patent regarding the use of this technique in an in-line fashion in internal combustion engines [26].

### *Hydrogen Sulfide (H<sub>2</sub>S) Detection*

Electrochemical sensors are the primary tools for H<sub>2</sub>S detection. Sulfur compounds can generally be converted to hydrogen sulfide via reductive pyrolysis, so a detection technique that can only function with H<sub>2</sub>S might still work with other compounds, provided that they can be made to undergo such a reaction [27]. Both Dräger (mentioned above in the context of sulfur dioxide detection) [28] and RKI [29] sell small, handheld hydrogen sulfide gas detectors that are reported to possess approximate LODs of 0.1 ppm and 2 ppm, respectively, via electrochemical sensing.

### *Simultaneous Detection of Multiple Sulfur Species*

Buck Scientific sells a multi-sulfur species detector that is reported to possess an LOD of 0.2 ppm via flame photometry detection (FPD) [30]. This is the same technique upon which ASTM D6228 [31] is based. While this self-contained device is a larger benchtop unit, stand-alone FPD-based detectors, such as those sold by Agilent [32] and OI Analytical [33], would be smaller, at least before the addition of instrumentation capable of separation and/or combustion steps prior to analysis. While the ability to detect multiple sulfur species might be considered a disadvantage in the present application (as it would simply convolute the desired analysis), the implementation of a combustor prior to the detector would allow for the detection of only one species, such as SO<sub>2</sub>. Interestingly, however, it would appear that flame photometry does not

produce a linear instrument response to sulfur [34], which means its suitability in the present work may depend upon how quantitative results need to be.

### Indirect Sulfur Detection

Because  $\text{SO}_x$  compounds can be decomposed into sulfur and oxygen by electrochemical reduction, it might be possible to repurpose COTS oxygen sensors to indirectly detect  $\text{SO}_x$  compounds [35]. This would, of course, be prone to errors associated with other sources of oxygen, and the limits of detection of such a technique would be reliant upon the oxygen sensor itself.

In general, because sulfur can poison certain catalytic chemical processes, it might be possible to design a sensor that makes use of that poisoning as the detection mechanism [36]. One would, however, need to find some way of reliably recovering the catalyst for repeated measurements. Also, without specifying which catalytic process is being poisoned, it is difficult to predict the potential limits of detection.

### Mid-infrared and Near-infrared Spectroscopy for Measurement of Sulfur in Liquid-phase Fuel

There is evidence that sulfur can be measured directly in liquid-phase fuels using mid-infrared (MIR) absorbance data. S-H stretching modes corresponding to thiols can be detected between  $2,600\text{--}2,540\text{ cm}^{-1}$  with little direct interference from other vibrational modes, and C-S stretching modes corresponding to thiols, as well as both aliphatic and aromatic sulfur-containing compounds, can be detected between  $750\text{--}570\text{ cm}^{-1}$  (spectral data found in the latter wavenumber range can additionally indicate the presence of both sulfate and sulfite ions).<sup>1</sup> A visual representation of these wavelength ranges is shown in Figure 1 (from Socrates [37]) to illustrate detection potential.

This information indicates that MIR data would be well-equipped to predict sulfur contents in fuels. Existing literature [38, 39] on the topic of sulfur detection in crude oils serves as further indirect evidence of this utility. Also, because the near-infrared (NIR) spectral region ( $\sim 13,000\text{--}4,000\text{ cm}^{-1}$ ) can reveal overtone bands of the types of fundamental modes found the  $2,600\text{--}2,540\text{ cm}^{-1}$  region [40], there is every reason to suspect that NIR data could also be used to detect these compounds. A small-scale study conducted by Wagner et al. [41] using 35 jet fuel samples seemed to indicate this feasibility as well, and specifically indicated the utility of a narrower NIR spectral range spanning from  $10,000\text{--}6,250\text{ cm}^{-1}$  which can be assessed using relatively inexpensive NIR hardware.

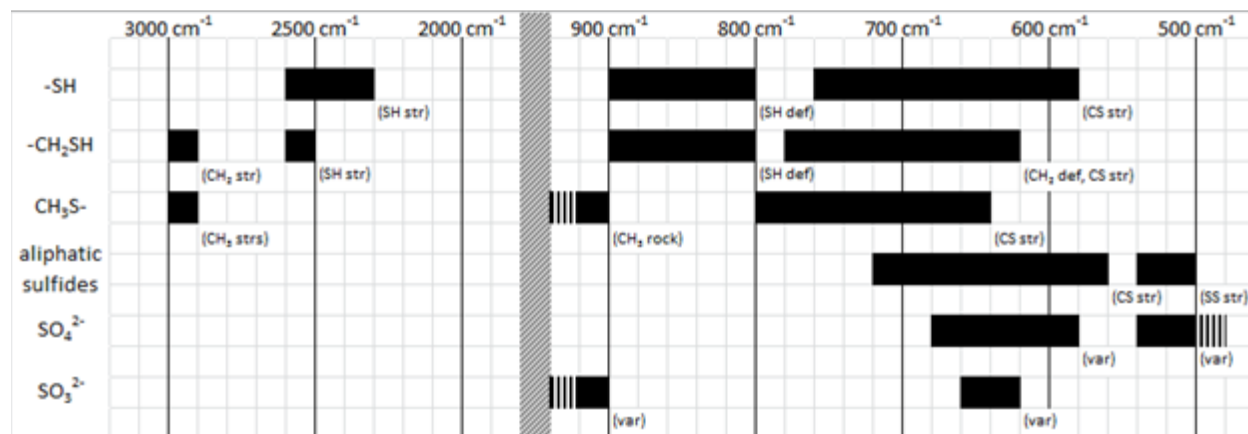


Fig. 1: Visual representation of vibrational mode frequency ranges for various sulfur-bearing compounds (from Ref. 37).

## Cermet Sensors and Cyclic Voltammetry

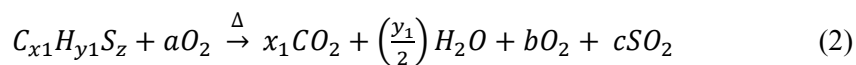
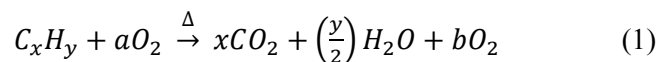
Electrochemical sensors composed of a ceramic–metallic (cermet) solid electrolyte have previously been studied for the detection of gaseous sulfur compounds SO<sub>2</sub>, H<sub>2</sub>S, and CS<sub>2</sub> in a study involving 11 toxic industrial chemical (TIC) compounds [42, 43]. The cermet sensors themselves are currently designed for vapor-phase detection and therefore any fuel mixture being tested would need to be vaporized in some manner. This could be achieved by simply heating the fuel, similar to the procedure for gas chromatography, or by combusting the fuel. Simple heating of the fuel would leave the organosulfur compounds in their original form, but the complex mixture could prove difficult to analyze. Combustion of the fuel, meanwhile, would result in a simpler mixture with SO<sub>2</sub> as the main sulfur-containing compound. The challenge for either method is to correlate the signal response to ppm levels of sulfur in liquid fuel.

## Optical Methods for Measurement of Sulfur in Combustion Exhaust Gas

The majority of sulfur in a fuel is converted to SO<sub>2</sub> when the fuel is burned in an oxygen-rich environment, as discussed in the next section. There are several optical methods that can be used to detect and quantify SO<sub>2</sub>, including flame photometry, chemiluminescence, and UV fluorescence. These methods are commonly used in commercial SO<sub>2</sub> sensors and gas chromatography, and were reviewed in a previous NRL letter report [44]. Generally, flame photometry is unlikely to have sufficient sensitivity for this application, in which it is necessary to quantify sulfur levels below 10 ppm. The chemiluminescence method is complicated in that it requires reaction with ozone to produce excited-state SO<sub>2</sub>. Therefore, in this study we will assess the UV fluorescence method carefully and determine if it has sufficient sensitivity and ease of implementation. After combustion in an oxygen-rich environment, SO<sub>2</sub> fluoresces in the 320 nm – 340 nm region, and the signal can be enhanced by first exciting SO<sub>2</sub> with a xenon lamp. Another technique, commonly used in measurements of engine exhaust, is non-dispersive infrared (NDIR) detection. This method takes advantage of the absorption of a specific infrared wavelength, which is proportional to species concentration, and the existence of COTS NDIR-based SO<sub>2</sub> detectors speaks to its viability in the present context. We evaluated both NDIR and UV fluorescence in this program.

## Conversion of Sulfur to SO<sub>2</sub> via Combustion

All sulfur in a liquid fuel converts to SO<sub>2</sub> and SO<sub>3</sub> when the fuel is burned with oxygen or air, though only a small fraction is SO<sub>3</sub> in most cases. For the purposes of this discussion, it is assumed that all sulfur converts to SO<sub>2</sub> during combustion. Any discrepancy between actual measured SO<sub>2</sub> and expected SO<sub>2</sub> based on the “full conversion” assumption could likely be accounted for with a small correction factor. To understand the relationship between sulfur in fuel and SO<sub>2</sub> generated during combustion, a reaction model was developed in MATLAB, using the following equations:



Equation 1 details the idealized combustion process between a fuel with  $x$  carbon atoms and  $y$  hydrogen atoms and amount  $a$  of oxygen. The constant  $a$  depends on the type of fuel being used and the amount of excess oxygen,  $b$ . Equation 2 details the idealized combustion process of a sulfur compound in the fuel with oxygen. The amount of sulfur in the fuel is typically orders of magnitude smaller than the amount of fuel being burned, thus it was helpful to decouple the reactions. A key consideration in these calculations is the assumption of excess oxygen in the reactant stream, meaning that the combustion is fuel-lean. Lean combustion is preferred because it produces lower levels of soot and NO<sub>x</sub>.

Assuming a fuel sulfur mass/weight concentration of 100 ppm and a fixed proportion of excess oxygen, we calculated the expected SO<sub>2</sub> concentration for each of the four sulfur compounds chosen for this study, which are shown in Figure 2 (DTBDS; 2-HTP; 3-MBTP; and 4,6-DMDBTP) in a later section of this report, in two different single-component fuels: dodecane (C<sub>12</sub>H<sub>26</sub>) and tetradecane (C<sub>14</sub>H<sub>30</sub>). Results are shown in Table 2, with SO<sub>2</sub> concentrations reported as volume fractions since exhaust gas analyzers typically report concentrations this way.

Table 2: Expected SO<sub>2</sub> concentrations (by volume) in combustion exhaust, assuming 100 ppm (by weight) of the various sulfur compounds in either dodecane (C<sub>12</sub>H<sub>26</sub>) or tetradecane (C<sub>14</sub>H<sub>30</sub>) fuel.

Sulfur compound	SO <sub>2</sub> concentration, by volume [ppm]	
	C <sub>12</sub> H <sub>26</sub> combustion	C <sub>14</sub> H <sub>30</sub> combustion
DTBDS	4.01	4.02
2-HTP	4.01	4.02
3-MBTP	4.01	4.02
4,6-DMDBTP	4.01	4.02

The calculations revealed some interesting details. First, the production of SO<sub>2</sub> during combustion appears to be independent of the sulfur compound chemistry. As seen in Table 2, using four different sulfur compounds results in the same concentration of SO<sub>2</sub> in the exhaust. Second, expected SO<sub>2</sub> concentration is independent of the type of fuel, at least for hydrocarbon fuels. Dodecane has two fewer carbon atoms and fourteen fewer hydrogen atoms than tetradecane. Regardless of the sulfur compound, however, the SO<sub>2</sub> concentrations expected for combustion of the two fuels differ by less than 0.25%. In addition, the results in Table 2 show that the concentration of sulfur in the fuel is nominally two orders of magnitude higher than the concentration of SO<sub>2</sub> in the exhaust. Thus, in order to measure 10 ppm of sulfur in a fuel, the SO<sub>2</sub> produced in stoichiometric conditions would be 0.4 ppm (400 parts per *billion*, ppb). This is a level of sensitivity that is difficult to achieve in standard exhaust gas analyzers.

## OBJECTIVE

The primary objective of this work was to evaluate methods for in-line detection and quantification of sulfur at sub-10-ppm levels in mobility fuels and to identify the best option based on convenience, cost, and ease of implementation. It was assumed that any required instrumentation would need to be reasonably small and field-deployable.

## INFRARED SPECTROSCOPY FOR DIRECT LIQUID-PHASE ANALYSIS

### Experimental Setup

#### *Spectrophotometer*

A Bruker Vertex 70 spectrophotometer was used to investigate the spectral features in several model organosulfur compounds. The instrument was configured to encompass the spectral range of 11,450 cm<sup>-1</sup> to 50 cm<sup>-1</sup>. A Pike Technologies MIRacle attenuated total reflectance (ATR) accessory with a zinc selenide crystal sampling surface was employed to acquire spectral data across the entire spectral range of the instrument. The relatively short path length of the infrared light penetration into the sample from the ATR sampling surface allowed for more consistent, less noisy data that was well-suited for multivariate data modeling.

In addition to the ATR accessory, quartz cuvettes (Heraeus Quarzglas Suprasil) were used in some experiments to provide a longer path length, potentially enhancing sensitivity, over a spectral range down to  $2,000\text{ cm}^{-1}$ . However, investigations undertaken during the present work indicated that the use of longer path lengths also resulted in peak broadening effects that, in turn, tended to obscure sulfur-based data features in a manner that could not be mitigated through other means. This is why the ATR is employed for the majority of the work seen in this report. Potassium bromide (KBr) salt plates were also used to evaluate samples at wavenumbers as low as  $500\text{ cm}^{-1}$ .

At one time, Bruker Optics also produced a rugged NIR-based fuel analyzer referred to as the “FuelEx”. In our evaluation of the FuelEx during the course of the present work, it was determined that this instrument was not more capable of detecting organosulfur compounds in fuels than the Vertex 70. Therefore, the FuelEx was considered redundant and the Vertex 70 spectrophotometer was used in this work.

### *Data Processing and Preprocessing*

Data collected during the present work were imported into MATLAB and subjected to both a baseline correction and a unit area normalization on the absorbance spectra, a methodology developed during previous work in our laboratory to account for minor instrument drift effects in infrared data, unless otherwise noted in the text. Data preprocessing and Partial Least Squares (PLS) regression modeling were conducted using functionality provided by the PLS\_Toolbox for MATLAB.

## **Results and Discussion**

### *Initial NIR/IR Organosulfur Compound Survey*

The four model organosulfur compounds shown in Figure 2 were selected for the initial evaluation of spectral properties. These model compounds consisted of a disulfide, an aliphatic thiophene, and a mono- and di-aromatic thiophene. Although these four compounds do not provide S-H stretching mode information, the literature [41] indicates that sulfides, despite being the explicit target of a fuel-based diagnostic test for such compounds (ASTM D3227), are not considered to be a major component of the organosulfur compounds in typical mobility fuels. Nonetheless, a fifth sulfide compound, 1-pentanethiol, was also evaluated to a limited extent to predict whether or not such compounds would behave in a significantly different fashion than the four model compounds. Near-infrared (NIR) and infrared (IR) data were collected from these four neat compounds, using KBr pellets for the solid 4,6-dimethyldibenzothiophene and the ATR accessory for the three remaining liquid compounds. Spectra were collected in several sequential segments to accommodate instrumental limitations when using the ATR accessory and aligned afterwards.

The results of this initial survey are shown in Figures 3 through 6. The infrared spectra acquired from the pure organosulfur compounds were confirmed, at least to the extent possible, through literature references evaluating the same or similar compounds [45-48]. Figures 3 through 6 show that carbon-sulfur stretching vibrations, which are the only sulfur vibrational modes possessed by all four of the organosulfur compounds shown in Figure 2, appear at slightly different wavenumbers for each compound, which makes sense, as the structural variations of these sulfur-containing compounds would be expected to exhibit different vibrational modes. The fact that multiple sulfur-containing compounds possess multiple relevant vibrational modes provides additional evidence of the potential utility of both multivariate data modeling and the less chemically specific combination and overtone bands found in near-infrared spectra. The multiple out-of-plane vibrational modes found in 4,6-dimethyldibenzothiophene are most likely due to the presence of multiple ring types.

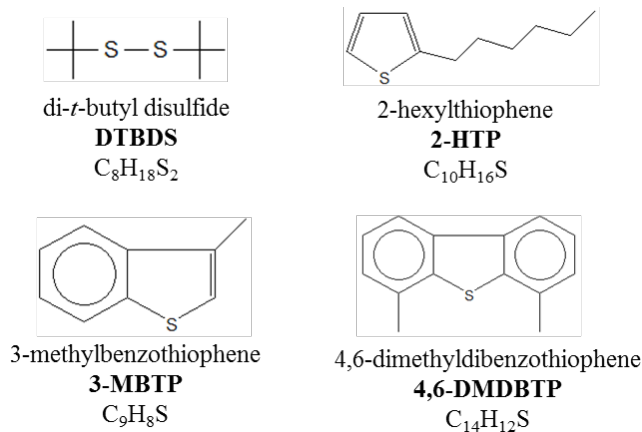


Fig. 2: Model organosulfur compounds examined in this study.

Hypothetically, areas of interest for further analysis would be those portions of the spectral range that display absorbance features indicative of the presence of organosulfur compounds. Visual examination of Figures 3 through 6 suggests that sulfur-specific vibrational modes for these four organosulfur compounds occur between 550 and 1000  $cm^{-1}$ , a circumstance that can be further confirmed by consulting Figure 1. In aggregate, these figures also seem to indicate that there is little to be gained from explicitly modeling data obtained at higher wavenumbers, at least until combinations and overtones make themselves apparent in the near-infrared range.

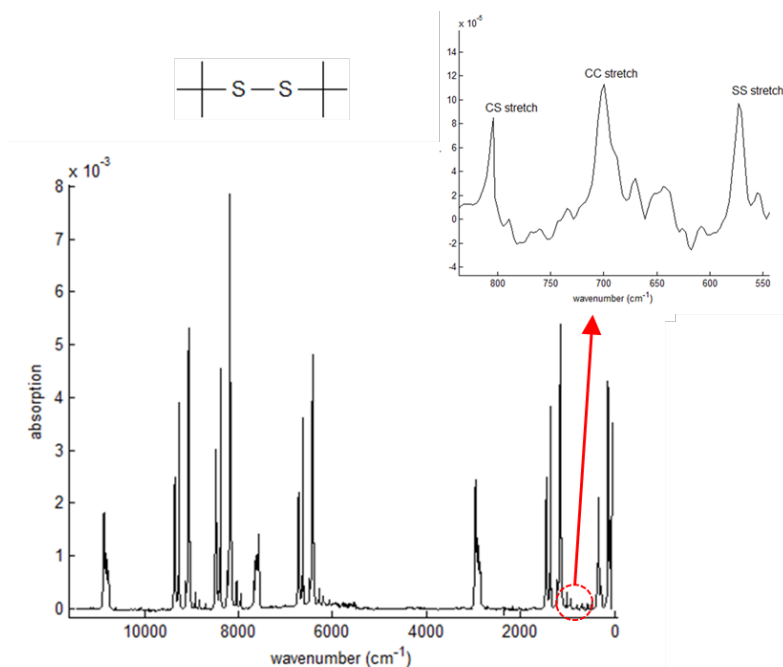


Fig. 3: Infrared absorbance spectrum of neat di-*t*-butyl disulfide, showing C-S, C-C and S-S stretching modes at about 800  $cm^{-1}$  and 550  $cm^{-1}$ , respectively.

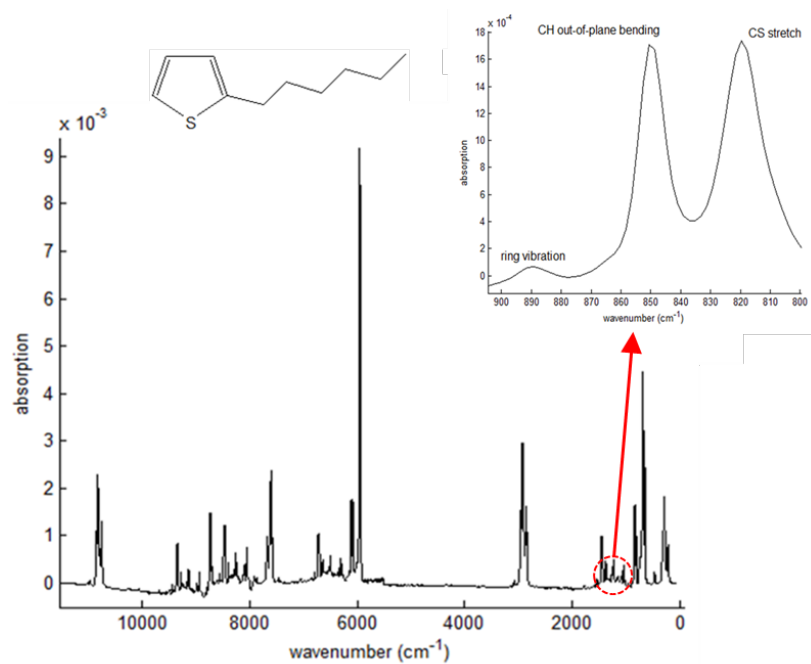


Fig. 4: Infrared absorbance spectrum of neat 2-hexylthiophene, showing the C-S stretching mode at about 815  $\text{cm}^{-1}$ .

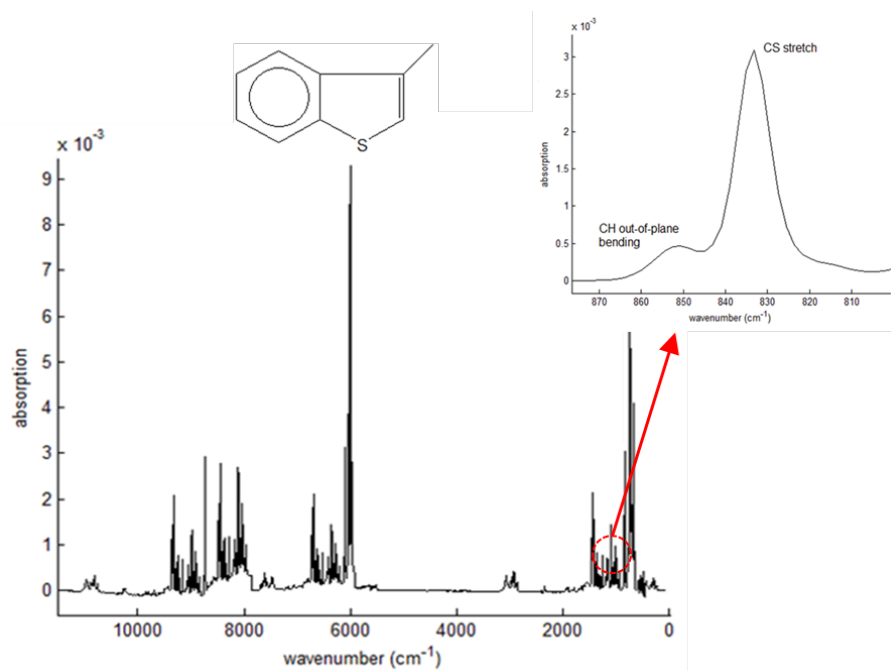


Fig. 5: Infrared absorbance spectrum of neat 3-methylbenzothiophene, showing the C-S stretching mode at about 835  $\text{cm}^{-1}$ .

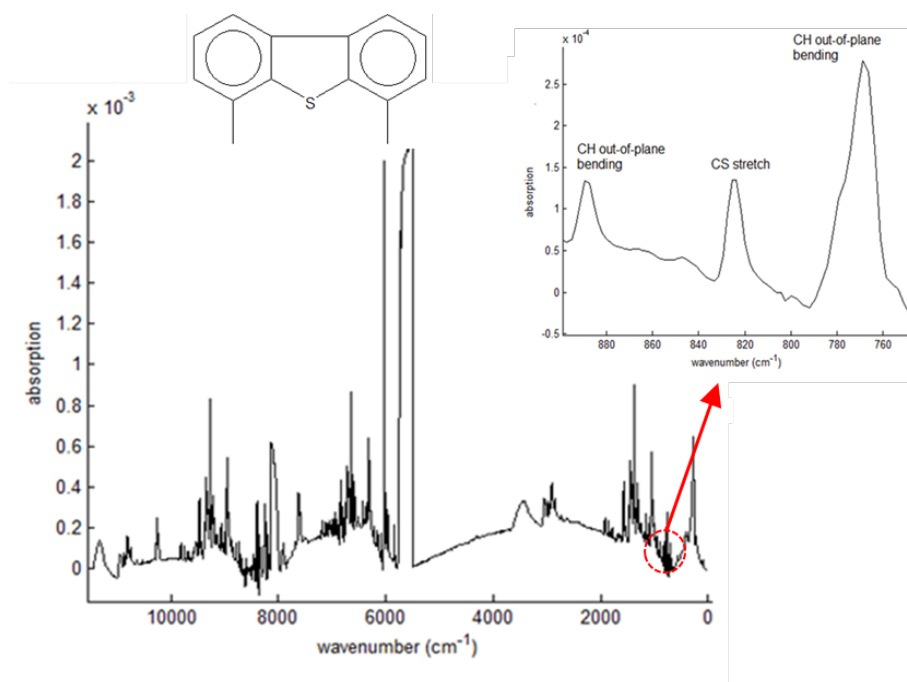


Fig. 6: Infrared absorbance spectrum of neat 4,6-dimethyldibenzothiophene, showing two C-H out of plane bending modes at about 770  $\text{cm}^{-1}$  and 890  $\text{cm}^{-1}$  and the C-S stretching mode at about 825  $\text{cm}^{-1}$ .

### *Fuel Surrogates*

Infrared spectra were acquired from samples of neat, i.e. pure, n-dodecane ( $\text{C}_{12}$ ), a surrogate jet fuel, and tetradecane ( $\text{C}_{14}$ ), a surrogate diesel fuel, using the ATR accessory. As expected, both hydrocarbons exhibited virtually identical infrared absorbance spectra, which can be seen as an extreme overlap in the data shown in Figure 7. It is primarily because of this apparent similarity that further data modeling and visual assessments only utilized dodecane.

The infrared spectra found in Figures 3 through 7, when considered together, indicate that there is little in the way of a reliable wavenumber range that would reveal the presence of all four sulfur-containing compounds without also inviting interferences from the vibrational modes inherent in even simple surrogate fuels. However, the NIR range of  $\sim 10,000\text{--}8,000\text{ cm}^{-1}$  ( $1,000\text{--}1,250\text{ nm}$ ) encompasses the range between the large surrogate interferences at  $10,800\text{ cm}^{-1}$  and  $7,600\text{ cm}^{-1}$  while maintaining only two smaller interferences in between, which is considered an adequate tradeoff for the purposes of multivariate data modeling. This range can be further extended to  $11,450\text{--}8,000\text{ cm}^{-1}$ , as far into the near-infrared as the instrumentation will allow, to take into account the known potential for NIR data to convey meaningful compositional information across multiple wavelengths simultaneously, i.e., covariance [49]. Also, the entire wavenumber range of  $1,250\text{--}50\text{ cm}^{-1}$  will be included in both visual data assessments and data modeling operations because this wavelength range is shown to encompass known C-S and S-S vibrational modes.

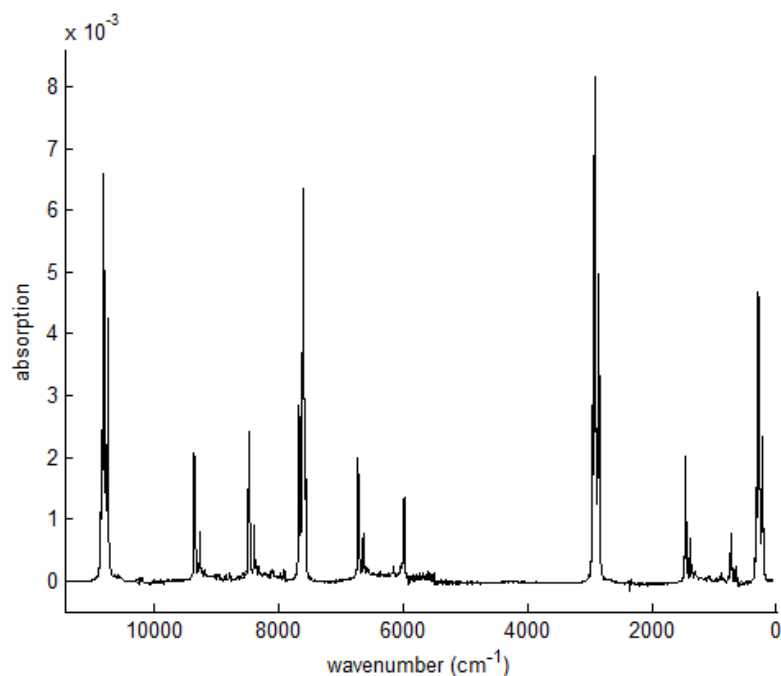


Fig. 7: Full-spectrum absorbance of neat surrogate fuels obtained with the ATR accessory.

#### *Extreme Fuel Surrogate/Organosulfur Compound Blending*

To illustrate prominent sulfur-relevant spectral features in sulfur-doped fuel samples, a blend of roughly 50% each of dodecane and DTBDS was created. The ATR-based data collected from this sample were not preprocessed in order to better show the relevant details. The sulfur vibrational modes between 500 and 850  $\text{cm}^{-1}$ , as indicated in Figure 3, are compared in Figure 8 with the same type of non-preprocessed data collected from the pure organosulfur compound and the neat surrogate fuel. Unsurprisingly, the sulfur-based vibrational modes in the ~50/50 sample possess roughly half of the intensity that they possess in the pure sulfur compound, and these same modes disappear completely in the neat surrogate fuel. Additionally, the large central peak, representing carbon-carbon stretching, both increases in absorbance and shifts a small amount in frequency as expected in response to relative concentration changes.

This same combination of organosulfur compound and surrogate fuel was also used to produce a 5,000 ppm sample, which, while being lower in sulfur content than the ~50/50 blend, still possesses far more sulfur than is likely to be encountered in a specification fuel. The data from this sample, replacing the data from the ~50/50 sample produced previously, can be found in Figure 9. Unfortunately, the spectroscopic data from this 5,000 ppm sample overlaps with the neat surrogate fuel data almost completely, and the spectral features of the organosulfur compound are thus not visually apparent.

Because quartz cuvettes will not allow for the proper analysis of this range, salt plates were employed to reassess the vibrational modes of the 5,000 ppm sample. The preprocessed results obtained by using salt plates instead of the ATR accessory to recollect the data found in Figure 9 can be found in Figure 10. Once again, however, these results seem to indicate that sulfur would remain difficult to detect even if the ATR accessory were not employed. Although salt plate-induced baseline effects and other spectral artifacts could not be completely eliminated from Figure 10, enough spectral information can be reliably interpreted to show how closely the 5,000 ppm sample and the neat surrogate fuel overlap one another. It would thus

appear that the difficulties encountered in detecting sulfur-sulfur and carbon-sulfur stretches in infrared spectroscopy is a consequence of how weak [50] these vibrational modes are, and not due to limitations inherent in the instrumentation.

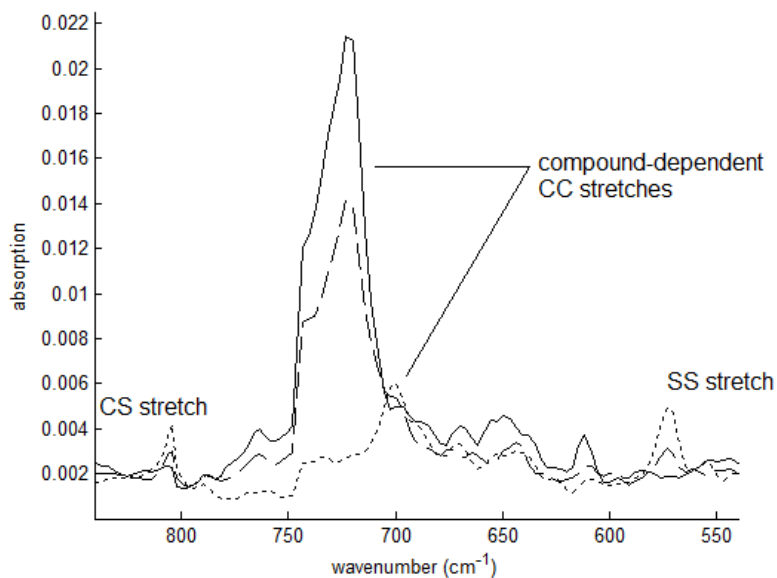


Fig. 8: Comparison of a sulfur-relevant range of absorbance results obtained from a pure organosulfur compound (small-dashed line), neat jet fuel surrogate (solid line), and a rough 50/50 blend of the two samples (long-dashed line).

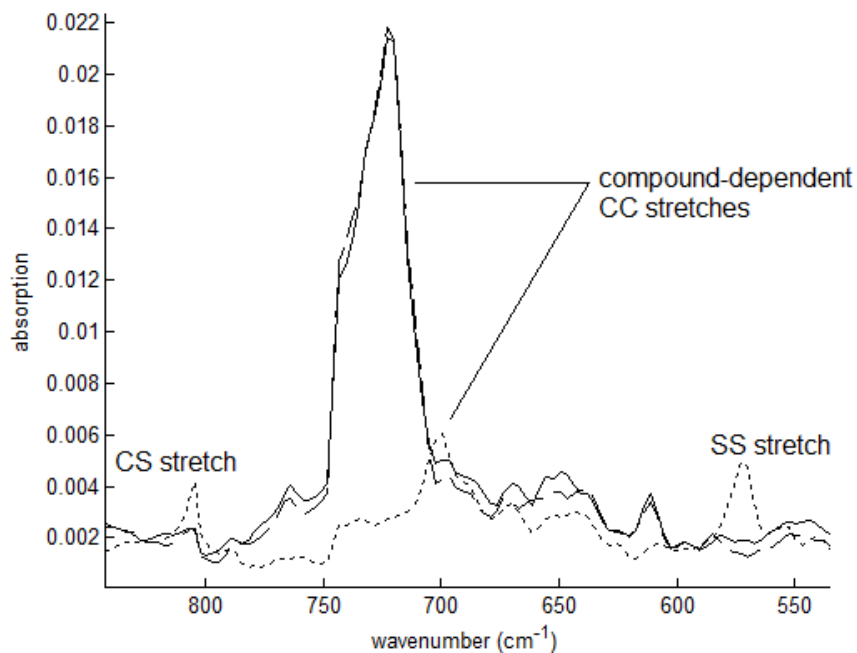


Fig. 9: The comparison seen in Figure 8, with the 50/50 blend replaced with a more modest 5,000 ppm sulfur blend (long-dashed line).

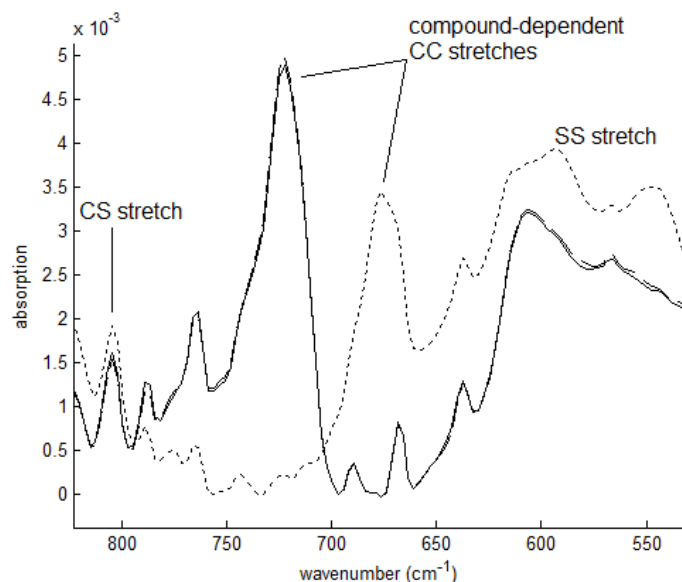


Fig. 10: Comparison of a sulfur-relevant range of absorbance results obtained from a pure organosulfur compound (small-dashed line), neat jet fuel surrogate (solid line), and a 5,000 ppm blend of the two samples (long-dashed line), all obtained through the use of salt plates.

A similar high sulfur concentration experiment was also performed with dodecane and 1-pentanethiol. A visual comparison of the S-H stretching mode obtained from ATR-IR measurements of the neat dodecane, pure 1-pentanethiol, and a 5,000 ppm blend is shown in Figure 11. Note that, similar to data shown in Figures 9 and 10, the neat surrogate fuel and the 5,000-ppm sample overlay each other so closely that any existing differences are more indicative of noise than compositional variance. This observation is consistent, again, with how weak S-H stretching modes are known to be [50], and seems to indicate that detecting thiols would be at least as challenging as detecting the four other organosulfur compounds to be considered in the remainder of the present work.

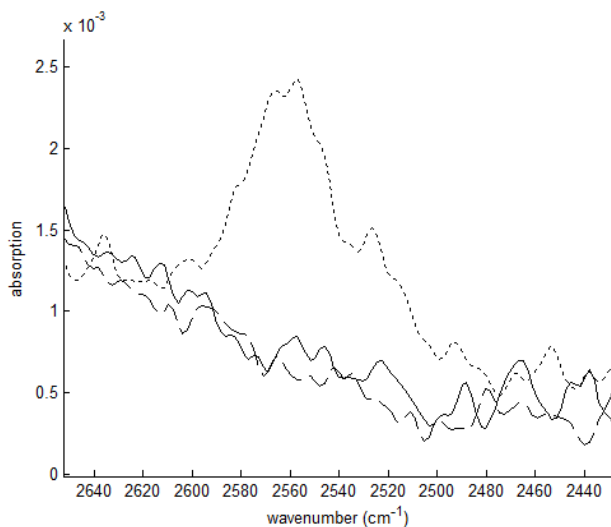


Fig. 11: Comparison of a sulfur-relevant range of absorbance results obtained from pure 1-pentanethiol compound (small-dashed line), neat jet fuel surrogate (solid line), and a 5,000 ppm blend of the organosulfur compound in the surrogate fuel (long-dashed line).

### *ATR NIR Multivariate Modeling*

NIR spectra were acquired with the ATR attachment from 11,450 to 8,000  $\text{cm}^{-1}$  (874 – 1250 nm) to model sulfur content using PLS regression. Resulting PLS models should, if chemically valid, be able to predict the sulfur content of an unknown sample from an infrared spectrum collected from that sample. Calibration samples were prepared in dodecane that contained 1, 10, 25, 100, and 500 ppm sulfur, from each of the four organosulfur compounds. Two replicate spectra were collected from each sample, and six blanks of neat dodecane were also collected.

The PLS models of sulfur content were evaluated in terms of Root Mean Square Error of Cross-Validation (RMSECV) results obtained from leave-one-out cross-validation (LOO) [51]. LOO is performed by predicting the sulfur content in each sample with a model constructed from every other sample. This technique indirectly ascertains model performance with uncalibrated samples not used to develop the model. The number of latent variables (LVs), the underlying linear factors to which calibration data are converted for calibration purposes, for all quantitative prediction models were chosen automatically using a statistic called the F-test [52]. The F-test was applied to the cross-validation results of the PLS modeling with an 85% confidence interval as has previously been found to be optimal in our laboratory. The F-test, by limiting the number of LVs, protects against models that are too biased towards a specific set of calibration data, which renders models less effective when predicting the sulfur contents of uncalibrated data. A thorough analysis of this type of model bias, i.e. overfitting, can be found in previous work [53].

Once the RMSECV results were used to select an appropriate number of LVs, a non-cross-validated PLS model was constructed from the same calibration data, and both the original calibration data and separate validation data were then introduced to the model to produce diagnostic sulfur prediction results and non-cross-validated Root Mean Square Error of Prediction (RMSEP) results. Because of the relatively small number of samples used to calibrate some of these models, results were also produced using a single LV for each model when necessary. The limits of detection (LOD) reported in these tables indicate the lowest detectable concentrations of sulfur that could be detected without false positive results, i.e. sulfur-free samples predicted to contain sulfur. LOD results indicated as >500 ppm were those samples in which 500 ppm samples could not be differentiated from the sulfur-free samples. These results, shown in Table 3 for the NIR data, include prediction models consisting of both a single organosulfur compound and multiple organosulfur compounds to provide a thorough evaluation of sulfur detection capabilities. These results are all based on 1-LV models, which was also the size automatically selected using the F-test in all cases.

Many of the sulfur prediction models in Table 3 seem more capable of providing low limits of detection with the validating non-calibration data than the calibration data used to produce the models, which is unusual. However, the RMSEP results clearly indicate the poor accuracy of the underlying prediction results, regardless of LOD. This poor accuracy is particularly troublesome when considering the single compound modeling, as these models should only require the uncovering of trends in five straightforward samples. These results indicate that NIR-based sulfur modeling cannot be used to reliably predict low organosulfur concentrations in realistically diverse fuels, though the scattered LODs of 1 found throughout the table might still indicate that NIR data can reliably detect sulfur in more limited capacities.

Table 3: Results of modeling sulfur content of model organosulfur compounds in dodecane from 11,450–8,000  $\text{cm}^{-1}$  (874–1,250 nm) using PLS regression of spectra acquired with ATR.

<b>Single Compound</b>				
calibration samples (5 samples each)	DTBDS	2-HTP	3-MBTP	4,6-DMDBTP
# calibration blanks	3	3	3	3
validation sample (5 samples each)	DTBDS	2-HTP	3-MBTP	4,6-DMDBTP
# validation blanks	3	3	3	3
#LVs	1	1	1	1
LOD (calibration), ppm	10	500	100	10
RMSEP (calibration), ppm	156	140	130	158
LOD (separate validation), ppm	N/A	500	1	1
RMSEP (separate validation), ppm	167	159	135	150
<b>Multiple Compounds</b>				
calibration samples (10 samples each)	4,6-DMDBTP 2-HTP 3-MBTP	4,6-DMDBTP 3-MBTP DTBDS	2-HTP 4,6-DMDBTP DTBDS	3-MBTP 2-HTP DTBDS
# calibration blanks	4	4	4	4
validation samples (10 samples each)	DTBDS	2-HTP	3-MBTP	4,6-DMDBTP
# validation blanks	2	2	2	2
#LVs	1	1	1	1
LOD (calibration), ppm	500	>500	>500	>500
RMSEP (calibration), ppm	166	175	178	173
LOD (separate validation), ppm	N/A	500	25	1
RMSEP (separate validation), ppm	194	167	158	172

### *Quartz Cuvette NIR Multivariate Modeling*

The use of quartz cuvettes in the Vertex 70 produces NIR spectral artifacts that do not seem to correspond to known compositional information, and the increased path length causes noticeable peak broadening effects. Figure 12 shows the normalized NIR spectra acquired from the same samples used to produce Table 3 with a 5-mm path length quartz cuvette over the wavelength range of 11,450–8,000  $\text{cm}^{-1}$  (874–1,250 nm). Baseline correction is not undertaken, however, because the staggered baseline shifts cannot be easily corrected for mathematically. Despite visual irregularities and a lack of obvious differences between the spectra regardless of sulfur concentration, PLS modeling was performed on these spectra to uncover any usable sulfur-relevant correlations that the increased path length might yield.

The PLS modeling results can be found in Tables 4 and 5, with the tables denoting the results obtained using the number of LVs determined by the F-test and a single LV, respectively. The longer path length of the 5 mm cuvette seemed to provide more consistent results than the ATR, as indicated by the lower RMSEP values. However, LODs do not generally improve regardless of the number of LVs employed, once again indicating that the NIR spectral responses of organosulfur compounds are simply too weak to provide sufficient sensitivity for the reliable detection of low sulfur concentrations in diverse fuels.

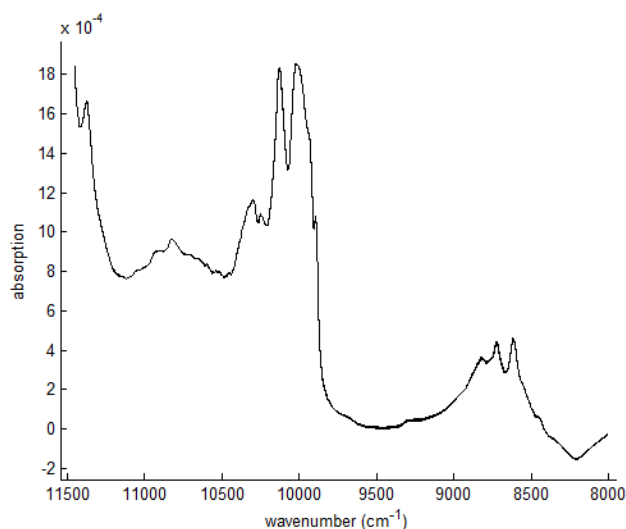


Fig. 12: NIR spectra acquired from the samples used to produce Table 3 using a 5-mm pathlength quartz cuvette.

Table 4: Results of modeling sulfur content of model organosulfur compounds in dodecane from 11,450–8,000  $\text{cm}^{-1}$  (874–1,250 nm) using PLS regression of spectra acquired from 5 mm quartz cuvettes.

<b>Single Compound</b>				
calibration samples (5 samples each)	DTBDS	2-HTP	3-MBTP	4,6-DMDBTP
# calibration blanks	3	3	3	3
validation sample (5 samples each)	DTBDS	2-HTP	3-MBTP	4,6-DMDBTP
# validation blanks	3	3	3	3
#LVs	1	2	2	2
LOD (calibration), ppm	>500	10	100	10
RMSEP (calibration), ppm	156	44	40	15
LOD (separate validation), ppm	>500	100	500	100
RMSEP (separate validation), ppm	172	43	54	21
<b>Multiple Compounds</b>				
calibration samples (10 samples each)	4,6-DMDBTP 2-HTP 3-MBTP	4,6-DMDBTP 3-MBTP DTBDS	2-HTP 4,6-DMDBTP DTBDS	3-MBTP 2-HTP DTBDS
# calibration blanks	4	4	4	4
validation samples (10 samples each)	DTBDS	2-HTP	3-MBTP	4,6-DMDBTP
# validation blanks	2	2	2	2
#LVs	6	5	6	5
LOD (calibration), ppm	10	100	100	100
RMSEP (calibration), ppm	5	32	24	35
LOD (separate validation), ppm	500	500	100	10
RMSEP (separate validation), ppm	199	157	46	84

Table 5: Results of modeling sulfur content of model organosulfur compounds in dodecane from 11,450–8,000  $\text{cm}^{-1}$  (874–1,250 nm) using PLS regression of spectra acquired from 5 mm quartz cuvettes, with 1 LV arbitrarily selected as the optimal number to use.

<b>Single Compound</b>				
calibration samples (5 samples each)	DTBDS	2-HTP	3-MBTP	4,6-DMDBTP
# calibration blanks	3	3	3	3
validation sample (5 samples each)	DTBDS	2-HTP	3-MBTP	4,6-DMDBTP
# validation blanks	3	3	3	3
#LVs	1	1	1	1
LOD (calibration), ppm	>500	25	1	25
RMSEP (calibration), ppm	156	152	144	67
LOD (separate validation), ppm	>500	1	100	500
RMSEP (separate validation), ppm	172	157	147	81
<b>Multiple Compounds</b>				
calibration samples (10 samples each)	4,6-DMDBTP 2-HTP 3-MBTP	4,6-DMDBTP 3-MBTP DTBDS	2-HTP 4,6-DMDBTP DTBDS	3-MBTP 2-HTP DTBDS
# calibration blanks	4	4	4	4
validation samples (10 samples each)	DTBDS	2-HTP	3-MBTP	4,6-DMDBTP
# validation blanks	2	2	2	2
#LVs	1	1	1	1
LOD (calibration), ppm	100	>500	>500	>500
RMSEP (calibration), ppm	100	147	162	174
LOD (separate validation), ppm	>500	500	100	>500
RMSEP (separate validation), ppm	221	170	159	171

### *Assessment of Modeling IR Spectra*

Results discussed above clearly illustrate the unresponsiveness of the combination and overtone bands in the NIR spectral range towards low concentrations of organosulfur compounds. In order to conduct a similarly thorough assessment of the applicability of the infrared spectral range known to at least potentially relay sulfur-relevant vibrational information more directly, PLS modeling identical to that performed on the NIR data was also conducted with IR spectra acquired from the range of 1,250–50  $\text{cm}^{-1}$  (8,000 – 200,000 nm). However, none of the models thus constructed were able to discriminate between the neat surrogate fuels and blends containing organosulfur contents as high as 500 ppm sulfur in their respective sets of validation data. This finding indicates that there is no advantage in using this infrared spectral range for sulfur content prediction modeling over the NIR range, despite the theoretical presence of sulfur-relevant data features in the former. Given the extreme blending results seen in Figures 8 through 11, it can be inferred that additional investigations of thiols would be likely to yield a similar result.

### **Conclusions**

The findings of this study indicate that infrared spectroscopy does not have sufficient sensitivity towards organosulfur compounds to constitute an acceptable detection method for sub-ppm levels of sulfur in Navy mobility fuels, at least in a general sense. However, NIR spectroscopy shows at least some utility in detecting individual organosulfur compounds, perhaps even to the desired limits of detection, in more limited circumstances, although such circumstances would seem to be somewhat contrived in the present context of a generalized detection technique suitable for diverse fuel populations.

One of the primary challenges of using infrared data to predict sulfur contents is the relative weakness of sulfur-based vibrational modes compared to the competing vibrational modes possessed by the compounds found in even simple surrogate fuels. The use of dual-beam instrumentation might be capable of at least partially mitigating this competition, but this would require the existence of a valid reference sample. Such a reference might exist if one were directly evaluating a fuel desulfurization strategy, as the post-desulfurization fuel could be used to mitigate the non-sulfur data features present in the pre-desulfurization fuel. However, this would likely not result in a detection strategy suitable for automation, as the identities of sulfur-relevant data features would need to be known *a priori* to understand the effects of a desulfurization strategy in their proper context.

## ELECTROCHEMICAL MEASUREMENTS OF SO<sub>2</sub>

### Cermet Sensors

#### *Experimental Setup*

Cermet sensors combine ceramic and metallic cells and have been used as electrochemical sensors for decades. There were 18 sensors available in house for testing in this program. The sensors are described in detail in previous work [42, 43], thus only a brief description is provided here. Each of the in-house cermet “sensors” is actually an array consisting of four sensors fabricated on a ceramic (Al<sub>2</sub>O<sub>3</sub>) substrate. Each of the four individual sensors of an array consists of an outer catalytic electrode and a lower electrode, both made of precious metals, with a solid electrolyte between them. Between the lower electrode and the ceramic substrate, there is a reference layer of Ni/NiO<sub>2</sub>, which provides a steady supply of oxygen that stabilizes the electrode for long-term use. The four sensors of each array have the following compositions:

- **Sensor A:** platinum (catalytic electrode) – yttria-stabilized zirconia (electrolyte) – platinum/palladium (lower electrode); abbreviated Pt–YSZ–Pt/Pd
- **Sensor B:** platinum – yttria-stabilized zirconia – platinum (Pt–YSZ–Pt)
- **Sensor C:** platinum – yttria stabilized zirconia – platinum with a tungsten bismuth oxide coating (Pt–YSZ–Pt–WBO)
- **Sensor D:** platinum – yttria stabilized zirconia – platinum/palladium with a tungsten bismuth oxide coating (Pt–YSZ–Pt/Pd–WBO).

In a typical test, a sensor array is operated at 250 °C. For cyclic voltammetry measurements, applied voltage is cycled over the range 0 mV to +1500 mV to –1500 mV to 0 mV (as a  $\pm$  triangular waveform) at a scan rate 400 mV/second (i.e., 15 seconds per cycle). To test a cermet sensor, the array is normally installed in a small enclosure (6 cm  $\times$  2.5 cm  $\times$  5.5 cm;  $\sim$ 82.5 cm<sup>3</sup>) through which test gas is circulated. Figure 13 shows a schematic of the experimental setup, specifically configured for dilute SO<sub>2</sub> measurements.

The SO<sub>2</sub> source is a cylinder of compressed gas consisting of 921 ppm SO<sub>2</sub> in a nitrogen (N<sub>2</sub>) balance. Using mass flow controllers, the dilute SO<sub>2</sub> gas can be further diluted with humidified (or dry) air, with total gas flow typically set to  $\sim$ 10 L/min (liters per minute). A separate mass flow controller is used to deliver a flow of  $\sim$ 10 L/min of humidified (or dry) air to purge the sensor enclosure and zero the sensor array. For both the SO<sub>2</sub>/N<sub>2</sub>/air mixture and the clean air, a vacuum pump is used to pull  $\sim$ 100 mL/min from the main flow and through the sensor enclosure.

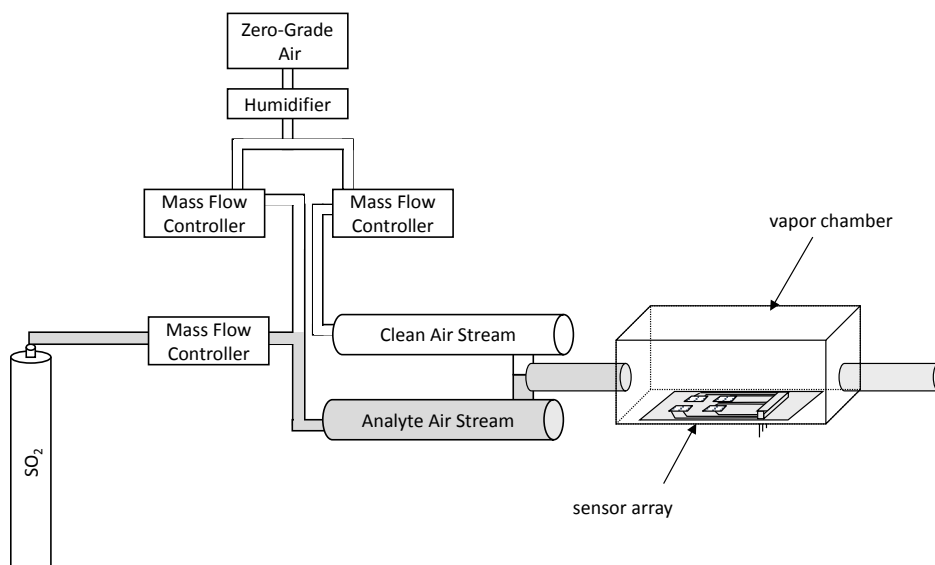


Fig. 13: Schematic of experimental setup for cermet sensor testing.

## Results and Discussion

An initial survey of the in-house sensors (i.e., arrays) was undertaken to determine which, if any, were still in working condition and suitable for this program. Of the 18 available sensors (i.e., arrays), 5 were found to be in good condition and providing some level of signal on all four elements/channels. Figure 14 shows example responses from the four elements of one of the working sensor arrays during a cyclic voltammetry cycle in which the sensor array was exposed to air.

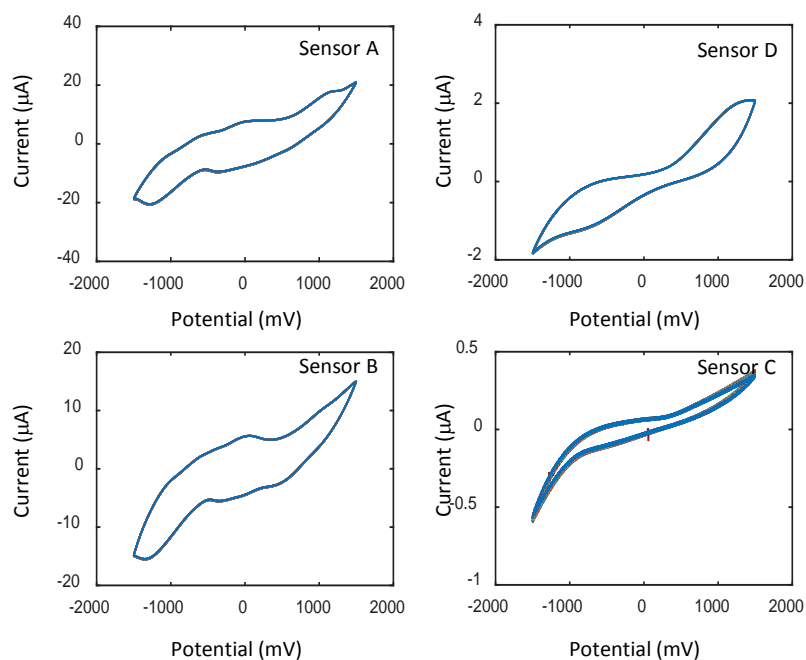


Fig. 14: Cyclic voltammogram curves for each of the four elements of a working cermet sensor array when exposed to air.

Initial testing was done with 5 ppm SO<sub>2</sub> in air to determine the effect on the response of the sensors. Of the 5 working sensor arrays, only 1 showed a significant response to SO<sub>2</sub>. Results for this sensor array are shown in Figure 15, where the plotted cermet “signal” has been background-subtracted, meaning that the sensor response (current) when exposed to air has been subtracted for the entire voltage cycle. The signal has also been unfolded, meaning that it has been plotted as a function of point number rather than as a function of voltage in the cycle. Finally, the signals for the four sensor elements/channels have been concatenated from left to right.

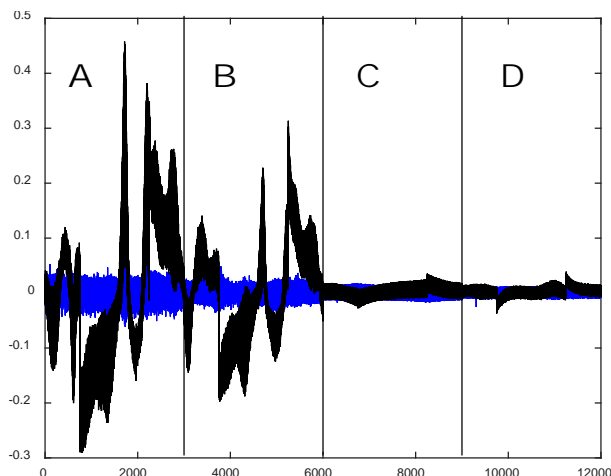


Fig. 15: Background-subtracted, unfolded, and concatenated cermet signal showing difference between response to clean air (blue) and response to 5 ppm SO<sub>2</sub> (black).

Sensor A shows a clear and substantial response to SO<sub>2</sub>, while Sensor B shows a clear but less substantial response. Sensors C and D show very little response to SO<sub>2</sub> at all. Thus, subsequent experiments focused on Sensor A of this single working cermet sensor array. Figure 16 shows the significance of the response of this sensor element to 5 ppm SO<sub>2</sub>, in terms of the first principal component (PC1) from principal component analysis (PCA).

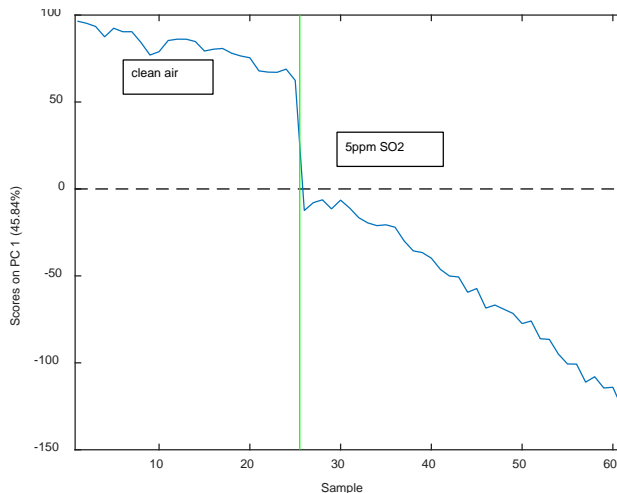


Fig. 16: Principal component analysis (PCA) plot showing clear response in PC1 (first principal component) to 5 ppm SO<sub>2</sub> exposure, even in the presence of sensor drift.

For each sample point in Figure 16, PCA was conducted and PC1 was determined for an entire cyclic voltammogram. Thus, each data point spans approximately 15 seconds, since that is the time required for completion of each voltage cycle. The test gas was changed from clean air to the mixture containing 5 ppm SO<sub>2</sub> at approximately 6 minutes after the start of the experiment, or at the point of sample # 25 in Figure 16. Even with a significant overall drift in the sensor response, the sudden change in response due to exposure to SO<sub>2</sub> is quite clear. These results suggested promise for using cermet sensors to measure SO<sub>2</sub> concentrations at the levels required for this program and justified further testing. The experimental plan included measurements of cermet sensor response to dilute SO<sub>2</sub> mixtures in air, followed by an assessment of cross-sensitivity to other species expected to be found in combustion exhaust, and finally measurements with actual combustion exhaust.

Experiments in which the cermet sensor was exposed to dilute SO<sub>2</sub> mixtures in air were expected to provide critical information about sensitivity, limit of detection, and repeatability. In this section, the term “sensor” refers to Sensor “A” of the sensor array that showed strong response to SO<sub>2</sub>. In the first experiment, the sensor was exposed to 4 ppm SO<sub>2</sub> three consecutive times, for approximately 3 minutes each time and with approximately 3 minutes between exposures to purge the sensor enclosure. Sensor response to these replicate exposures is shown in Figure 17, where the sensor “signal” is simply the sum of the response (i.e., electrical current) over the entire applied voltage cycle. The summed signal is a convenient and simple way to examine the sensor response, as well as sensor drift. As shown in Figure 17, the response to only 4 ppm SO<sub>2</sub> is significant and encouraging. Unfortunately, the signal decreased with each exposure, which would be problematic for determining quantitative SO<sub>2</sub> concentration if the trend were to persist. Since the cermet sensor had not been used in quite some time prior to these experiments, it is possible that the decreasing signal was a result of a “break-in” process.

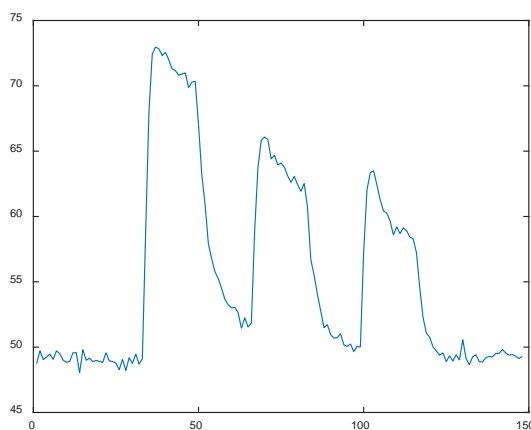


Fig. 17: Sensor response for three consecutive exposures to 4 ppm SO<sub>2</sub>. Abscissa (x-axis) value is sample number, and each sample spans an entire 15-second voltage cycle. Ordinate (y-axis) value for each point is the sum of the sensor response (electrical current) over an entire 15-second voltage cycle.

Next, a full run of measurements for varying SO<sub>2</sub> concentrations was conducted to examine detection limit, repeatability, and drift. The sensor was exposed to gas streams containing 0.2 ppm, 0.5 ppm, 1 ppm, 2 ppm, and 4 ppm SO<sub>2</sub> in a pattern of increasing, then decreasing, then increasing concentrations. Sensor response, again in terms of summed signal over the entire voltage cycle for each point, to the varying concentrations is shown in Figure 18. There are several important observations that can be made from these results. First, the signal was directly proportional to SO<sub>2</sub> concentration, which is encouraging. Second, the

signal for a given concentration decreased over time, similar to what was observed in Figure 17. At this point, it was not yet clear if this pattern would continue or if the sensor would reach a steady state. Finally, there was a sharp decrease in signal at the end of the experiment and the baseline response for exposure to air was significantly different at the end of the experiment than at the outset. The reason for this sudden baseline shift is unknown, as the raw voltammograms from the beginning and end of the experiment looked quite similar.

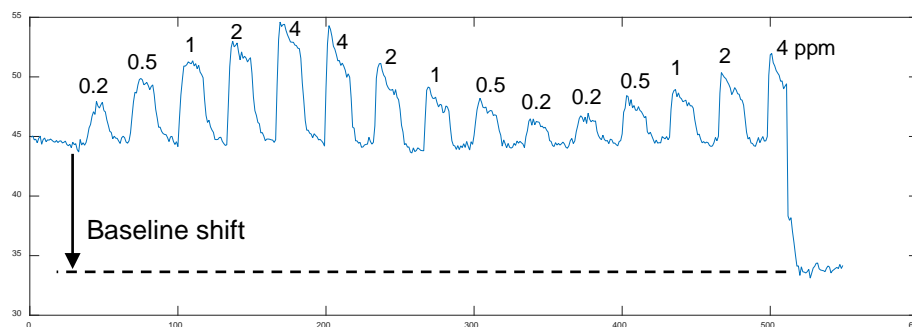


Fig. 18: Sensor response to SO<sub>2</sub> for 0.2 ppm, 0.5 ppm, 1 ppm, 2 ppm, and 4 ppm concentrations in an increasing-decreasing-increasing pattern. Abscissa (x-axis) value is sample number, and each sample spans an entire 15-second voltage cycle. Ordinate (y-axis) value for each point is the sum of the sensor response (electrical current) over an entire 15-second voltage cycle.

Issues with decreasing signal notwithstanding, the significant signal with respect to baseline even at the lowest SO<sub>2</sub> concentration of 0.2 ppm was encouraging. Thus, lower concentrations were tested in a subsequent experiment. This time, the sensor was exposed to 0.1 ppm, 0.25 ppm, 0.5 ppm, and 1 ppm, once each in ascending order. Sensor response, again in terms of summed signal over the entire voltage cycle for each point, to the varying concentrations is shown in Figure 19. In this experiment, again there was baseline shift, but this time at the outset rather than at the end. While there was some direct correlation between concentration and sensor response, the change in signal was much smaller. In fact, the differences in the signals for the 0.1 ppm, 0.25 ppm, and 0.5 ppm cases are difficult to discern at all.

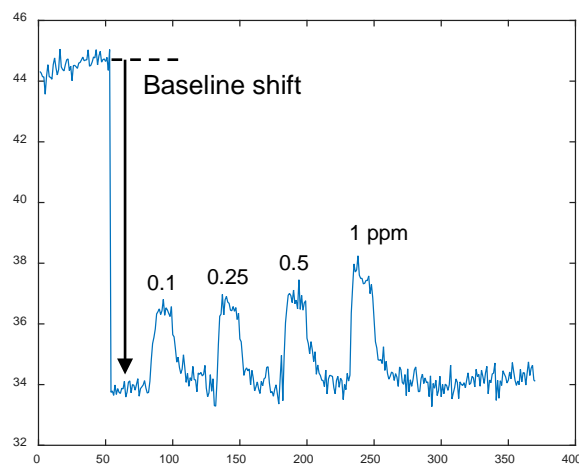


Fig. 19: Sensor response to SO<sub>2</sub> for 0.1 ppm, 0.25 ppm, 0.5 ppm, and 1 ppm concentrations, in ascending order. Abscissa (x-axis) value is sample number, and each sample spans an entire 15-second voltage cycle. Ordinate (y-axis) value for each point is the sum of the sensor response (electrical current) over an entire 15-second voltage cycle.

The next step was to measure the sensor response for repeated exposures to these very low SO<sub>2</sub> concentrations, to determine if the smaller response was due to a legitimate issue with the sensor. For this experiment, the sensor was exposed to 0.1 ppm, 0.25 ppm, 0.5 ppm, 1 ppm, 2 ppm, and 4 ppm SO<sub>2</sub>, each in triplicate. Sensor response, again in terms of summed signal over the entire voltage cycle for each point, to the varying concentrations is shown in Figure 20. The signal, while still showing a slight increase with increasing SO<sub>2</sub> concentration, still seemed to be degrading overall. The difference in signal between 0.1 ppm and 4 ppm is clear, but differences between 0.1 ppm and 0.25 ppm or between 2 ppm and 4 ppm are not at all clear.

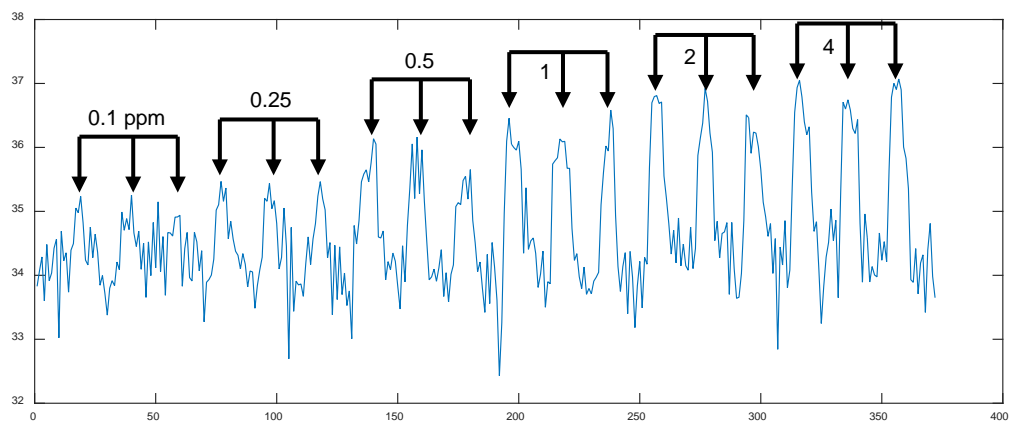


Fig. 20: Sensor response to SO<sub>2</sub> for 0.1 ppm, 0.25 ppm, 0.5 ppm, 1 ppm, 2 ppm, and 4 ppm concentrations, in triplicate and in ascending order. Abscissa (x-axis) value is sample number, and each sample spans an entire 15-second voltage cycle. Ordinate (y-axis) value for each point is the sum of the sensor response (electrical current) over an entire 15-second voltage cycle.

Further evidence of a progressive issue with the sensor can be seen through examination of raw voltammograms. Shown in Figure 21 are two voltammograms recorded during air exposures, one (black trace) corresponding to baseline data from the initial sensor survey and the other (blue trace) corresponding to baseline data from the experiments relevant to Figure 20. The primary change in the voltammogram can perhaps best be described as a clockwise rotation, with the upper right corner of the trace having shifted downward and the lower left corner of the trace having shifted upward. In addition, the negative-voltage portion of the voltammogram became noticeably wider. The reasons for specific changes in the voltammogram are not known, but it is clear that the response of the sensor has changed after repeated exposure to SO<sub>2</sub>.

Though not discussed above in the “Experimental Setup” section, it was normal procedure at the end of an experimental run to heat the sensor array above the normal operating temperature of 250 °C to 310 °C for a 5-minute recovery period. After the series of experiments described above was complete, the sensor array was heated several times to an even higher temperature of 325 °C for extended periods of time. This was done in an attempt to revive the sensor and return it to a stable baseline. After the heating procedure, the sensor was again exposed to gas streams containing 0.2 ppm, 0.5 ppm, 1 ppm, 2 ppm, and 4 ppm SO<sub>2</sub> in a pattern of increasing, then decreasing concentrations. Sensor response, again in terms of summed signal over the entire voltage cycle for each point, to the varying concentrations is shown in Figure 22. The results show that the use of heating to revive the sensor was unsuccessful. The overall signal level was even lower than before and there was no apparent response of the sensor to SO<sub>2</sub> at all, regardless of concentration.

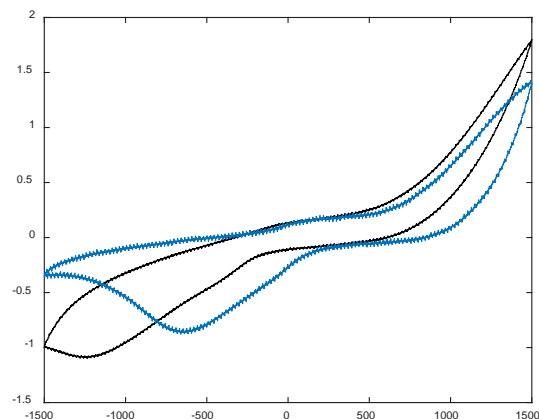


Fig. 21: Raw cyclic voltammograms for baseline air-exposure measurements from the initial sensor survey (black trace) and from experiments relevant to Figure 20 (blue trace).

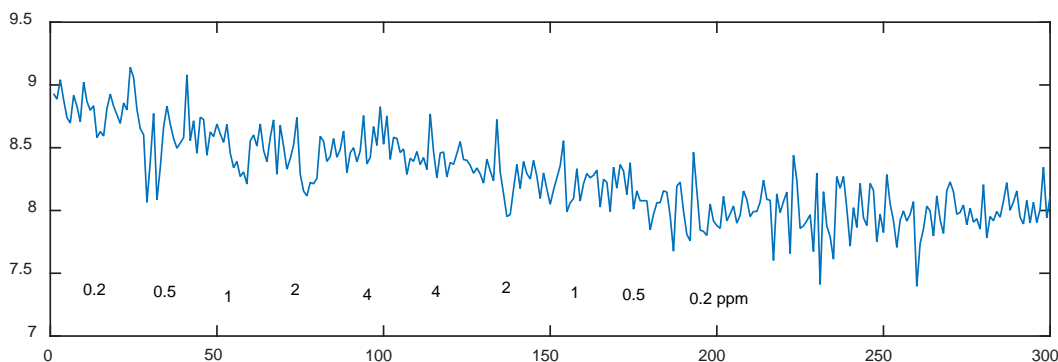


Fig. 22: Sensor response to  $\text{SO}_2$  for 0.2 ppm, 0.5 ppm, 1 ppm, 2 ppm, and 4 ppm concentrations in an increasing-decreasing pattern. Abscissa (x-axis) value is sample number, and each sample spans an entire 15-second voltage cycle. Ordinate (y-axis) value for each point is the sum of the sensor response (electrical current) over an entire 15-second voltage cycle.

## Conclusions

Despite the initial promise shown by the cermet sensors, in terms of the strong response of a sensor to  $\text{SO}_2$  and the positive correlation between concentration and signal, it appears that prolonged and repeated exposure to  $\text{SO}_2$  irreversibly degraded the sensor until it no longer responded to  $\text{SO}_2$  at all. Thus, it was not possible to continue testing with the cermet sensor to examine cross-sensitivity to specific combustion products or to examine response to real combustion exhaust gas.

It seems that this work could be pursued further by engaging with a company that can develop and manufacture new cermet sensors, such as General Atomics, or a research group with appropriate facilities and expertise such as those at Argonne National Laboratory. The primary challenge is identifying materials that respond to  $\text{SO}_2$  but are not degraded by it. If candidate materials can be identified and prototype sensors fabricated, initial testing would be required to verify sensitivity to  $\text{SO}_2$  and to examine cross-sensitivity to other combustion products.

## Commercial SO<sub>2</sub> Sensor

### Experimental Setup

Two Dräger PAC 7000 units, each equipped with a DrägerSensor XXS SO<sub>2</sub> sensor, were acquired for testing of commercial-off-the-shelf (COTS) electrochemical sensor systems. According to the manufacturer, these units can measure SO<sub>2</sub> concentration from 0 to 100 ppm with 0.1-ppm resolution. The stated operating temperature and humidity limits, which can be important for use in monitoring combustion exhaust gases, are -30 to 50 °C and 10 to 90 % relative humidity (RH).

As shown in Figure 23, the two Dräger sensors (serial numbers 167 and 168) were placed in a 4.1-liter acrylic chamber (15 cm × 15 cm × 16 cm), with the data loggers set for 10-second interval measurements. Test gases, including SO<sub>2</sub>, CO<sub>2</sub>, CO, NO, and zero-grade air from compressed-gas cylinders, were set up to flow through the chamber at ~10 L/min (liters per minute), equating to a complete turnover of the chamber volume every ~24 seconds. It was determined in preliminary experiments that humidity in the gas stream was crucial for proper sensor operation, thus the zero-grade air was humidified by bubbling it through a container of water. All gas flows were controlled by Sierra mass flow controllers.

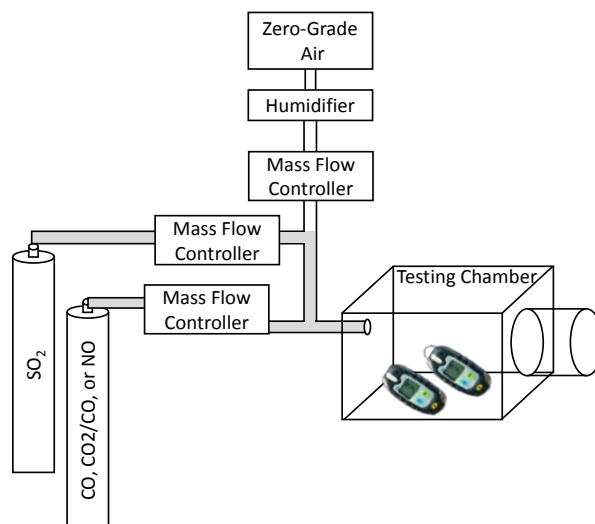


Fig. 23: Schematic of experimental setup for testing with Dräger SO<sub>2</sub> sensors.

### Results and Discussion

A standard test consisted of alternating exposure of the sensor to SO<sub>2</sub>/air mixtures and clean air. Mixtures with SO<sub>2</sub> concentrations of 0.2, 0.5, 1, 2, and 4 ppm (by volume) were tested multiple times, always in ascending order. Normally, the gases were humidified to approximately 25 % RH to ensure proper sensor behavior. For the first two sets of measurements with unit 167, however, the air was mistakenly left dry and not humidified. The sensor response was extraordinarily low (only ~10% of expected value), most likely due to the electrochemical sensor becoming too dry to allow for sufficient chemical reactivity. Thus, no data were recorded for unit 167 for these first two sets of measurements; once the mistake was discovered and corrected, however, data were collected for this sensor. Tests were also run to determine the effects of potential interfering species, as described in detail below. These tests did not appear to affect the long-term operation of the sensor or the response of the sensor to SO<sub>2</sub>. Results of all of the SO<sub>2</sub> exposure tests (not including interfering species tests) are shown in Figure 24.

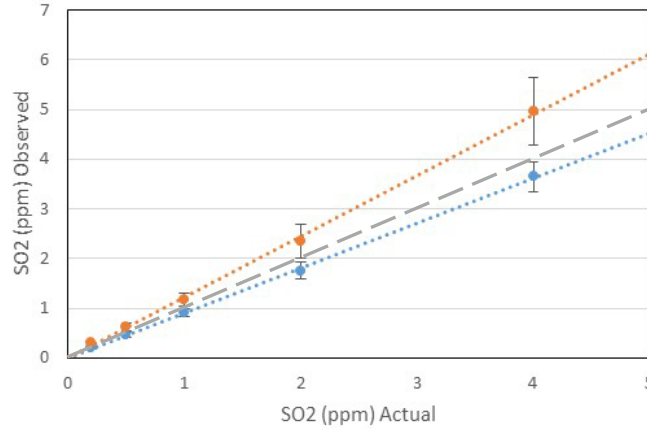


Fig. 24: Observed SO<sub>2</sub> concentrations vs. actual SO<sub>2</sub> concentrations over a 3-week period. Short-dashed lines indicate linear regression fits to the experimental data. The long-dashed gray line illustrates a perfect match between observed and actual SO<sub>2</sub> concentrations. Error bars represent  $\pm$  one standard deviation for the replicate measurements.

Figure 24 shows that the response from Unit 167 was generally higher than expected, while the response from Unit 168 was generally lower than expected, although it was encouraging that both had a highly linear and repeatable response to various SO<sub>2</sub> concentration levels. At the end of testing, both units were recalibrated using clean, humidified air (~25 % RH) for the zero level and a 5 ppm SO<sub>2</sub>/air mixture (~25 % RH) for a span level. When exposed to the 5-ppm SO<sub>2</sub> mixture, Units 167 and 168 read 5.67 ppm and 3.8 ppm, respectively. Both units were reset to 5 ppm and the exposure was repeated. After the recalibration, both units gave identical readings, but spot checks at various SO<sub>2</sub> concentrations showed that the readings were higher than the actual exposed SO<sub>2</sub> levels. This suggests that the response of these Dräger sensors is perhaps not reliable enough at these low concentrations to be practically useful for the intended application, in which it is necessary to quantify SO<sub>2</sub> concentrations < 1 ppm in combustion exhaust.

A potentially significant issue with COTS sensors, and one that we tested as described below, is cross-sensitivity to combustion gases. Table 6 shows the stated cross-sensitivities of the Dräger SO<sub>2</sub> sensors to gases relevant to combustion exhaust, as provided by the manufacturer. Based on this information, the only gas species of concern would be NO<sub>2</sub>, due to its noticeable effect on apparent SO<sub>2</sub> concentration. Exhaust from our combustor, however, is not expected to produce high levels of NO<sub>x</sub> species, and in particular should produce little to no NO<sub>2</sub> (i.e., nearly all NO<sub>x</sub> will be NO rather than NO<sub>2</sub>). It is noted, however, that combustion exhaust will contain much higher concentrations of some of the listed species. For example, CO<sub>2</sub> is expected to be ~10 vol. %, which is more than 6x the CO<sub>2</sub> concentration listed in Table 6. Therefore, it was necessary to examine cross-sensitivities in our test setup.

Table 6: Cross-sensitivity of DrägerSensor XXS SO<sub>2</sub> sensor to potential combustion exhaust gases.

Gas species	Concentration	Sensor response [ppm SO <sub>2</sub> ]
CO	200 ppm	No effect
CO <sub>2</sub>	1.5 vol. %	No effect
NO	20 ppm	No effect
NO <sub>2</sub>	20 pm	-30
CH <sub>4</sub>	1 vol. %	No effect

Several experiments were performed to assess cross-sensitivity, both with and without SO<sub>2</sub> in the gas mixture. All of the results, including SO<sub>2</sub> exposures without interfering species (i.e., results plotted in Figure 24), SO<sub>2</sub> exposures with interfering species, and exposures with no SO<sub>2</sub> and only interfering species, are shown in Table 7. As shown in the results for Run 5 and Run 8, inclusion of 10 ppm CO or 2 ppm NO in the background had no effect on the SO<sub>2</sub> measurements. A cylinder containing 8.48 % CO<sub>2</sub> and 0.87 % CO in a balance of N<sub>2</sub> was available, and when diluted with humidified air to CO<sub>2</sub> and CO concentrations of ~4000 ppm and ~400 ppm, respectively, the mixture had a noticeable effect on the SO<sub>2</sub> measurements.

Figure 25 shows the baseline shift caused by the background gas containing CO<sub>2</sub> and CO. The shift was ~1.5 ppm and 0.7 ppm on Units 167 and 168, respectively. In a subsequent experiment, the CO<sub>2</sub>/CO/N<sub>2</sub> gas mixture was tested without dilution (Run 10). The normal set of SO<sub>2</sub> runs was not conducted, but the presence of CO<sub>2</sub> and CO in the mixture resulted in significant sensor response. The false SO<sub>2</sub> readings were 31.2 ppm and 15 ppm for Units 167 and 168, respectively. It was determined that these false readings were due to the CO, as exposure of the sensors to pure CO<sub>2</sub> resulted in no measurable signal at all. The response of the Dräger sensors to CO is a major issue for use of these sensors to measure SO<sub>2</sub> in combustion exhaust, as this level of CO is a realistic concentration that could be found in typical exhaust gas.

Table 7: Summary of exposures and results of SO<sub>2</sub> and CO/CO<sub>2</sub>/NO testing for Units 167 / 168.

Run #	RH [%]	Interfering species	SO <sub>2</sub> concentration				
			0.2 ppm	0.5 ppm	1 ppm	2 ppm	4 ppm
1	25	--	-- / 0.2	-- / 0.4	-- / 0.8	-- / 1.6	-- / 3.2
2	25	--	-- / 0.2	-- / 0.5	-- / 0.9	-- / 1.9	-- / 3.2
3	25	--	0.3 / 0.3	0.5 / 0.5	1.0 / 1.0	1.9 / 1.9	3.9 / 3.9
4	25	--	0.3 / 0.2	0.5 / 0.5	1.2 / 0.9	2.4 / 1.7	4.9 / 3.4
5	25	CO 10 ppm	0.3 / 0.2	0.6 / 0.5	1.2 / 0.9	2.4 / 1.7	5.0 / 3.3
6	80	--	0.3 / 0.2	0.7 / 0.5	1.3 / 1.0	2.7 / 1.9	5.8 / 4.1
7	25	--	0.3 / 0.2	0.6 / 0.5	1.1 / 1.0	2.1 / 1.5	5.0 / 3.6
8	25	NO 2 ppm	0.2 / 0.2	0.5 / 0.3	1.0 / 0.7	2.0 / 1.4	4.7 / 3.3
9	25	CO <sub>2</sub> /CO 4000ppm/400ppm	1.7 / 0.9	2.0 / 1.1	2.7 / 1.7	3.7 / 2.2	6.3 / 4.0
10	75	CO <sub>2</sub> /CO 8.48%/0.87%	31.2 / 15.0 (no SO <sub>2</sub> runs)				
11	75	CO 1000 ppm	2 – 4 on both (no SO <sub>2</sub> runs)				
12	25	--	0.3 / 0.2	0.6 / 0.4	1.3 / 0.9	2.6 / 1.8	5.2 / 3.5
13	25	Recalibration	0.3 / 0.3	0.6 / 0.6	1.2 / 1.2	2.3 / 2.3	4.5 / 4.5

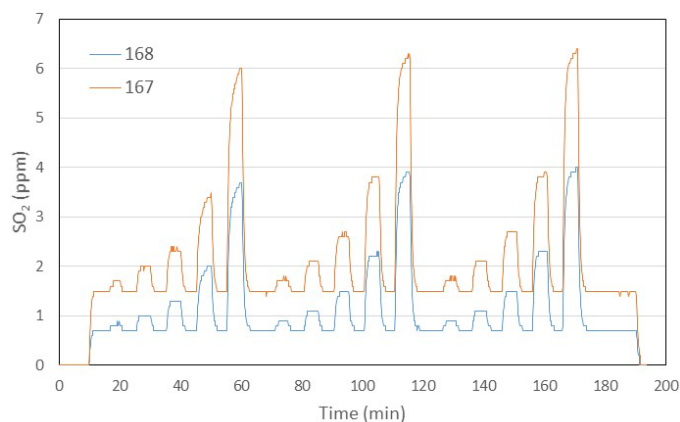


Fig. 25: Observed SO<sub>2</sub> concentrations in presence of humidified air containing ~4000 ppm CO<sub>2</sub> and ~400 ppm CO. Exposure to SO<sub>2</sub> was in a repeating pattern of 0.2 ppm, 0.5 ppm, 1 ppm, 2 ppm, and 4 ppm.

## Conclusions

In summary, although these COTS sensors initially appeared to show promise in terms of sensitivity to low levels of SO<sub>2</sub>, it appears that cross-sensitivity to species that are expected to be at significant levels in combustion exhaust gas could preclude their use. Testing with actual combustion exhaust gas was conducted, as described in a later section.

## OPTICAL MEASUREMENTS OF SO<sub>2</sub>

### Experimental Combustor Setup

A combustor was designed to burn small quantities of liquid fuel with air in a controlled environment that would enable SO<sub>2</sub> measurements using a variety of methods, including conventional exhaust gas analyzers, optical diagnostics, and electrochemical sensors. Figure 26 shows a photograph of the assembled combustor and Figure 27 shows the individual pieces of the assembly.

The combustion chamber is comprised of a stainless steel base with four stainless steel posts that have notches to hold steel and glass plates. The plates are interchangeable to enable flexibility, such as insertion of a plate with temperature instrumentation or insertion of additional glass plates for greater optical access to the flame. One of the steel plates has a hole near the bottom to position an air/fuel inlet and glow plug holder. The glow plug, an off-the-shelf unit that normally is used for cold ignition in diesel engines, serves as the ignition source for the combustor. The operating principle is simple – the tip becomes heated as a voltage is supplied. Air and liquid fuel flow in the small annular space between the glow plug and a stainless steel holder, and the liquid fuel vaporizes rapidly due to the high temperature. When the premixed air and fuel reach the tip of the glow plug, which is inside the combustion chamber, the mixture ignites and forms a small flame. The reaction produces exhaust gas that flows through the outlet at the top of the chamber. The glow plug was characterized to determine at what voltage JP-5 (military jet fuel) would ignite and over what voltage range a stable flame would be achieved. It was determined that flame stability was best for air flow rate of 2 L/min and fuel flow rate of 0.2 mL/min, which equates to an air-fuel ratio of approximately 13 (based on mass). Conditions for best flame stability change slightly for different fuels.

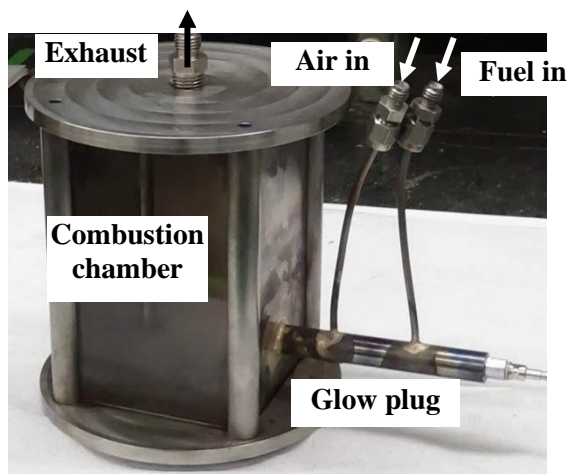


Fig. 26: Photograph of liquid-fuel combustor developed to measure SO<sub>2</sub> in combustion exhaust.

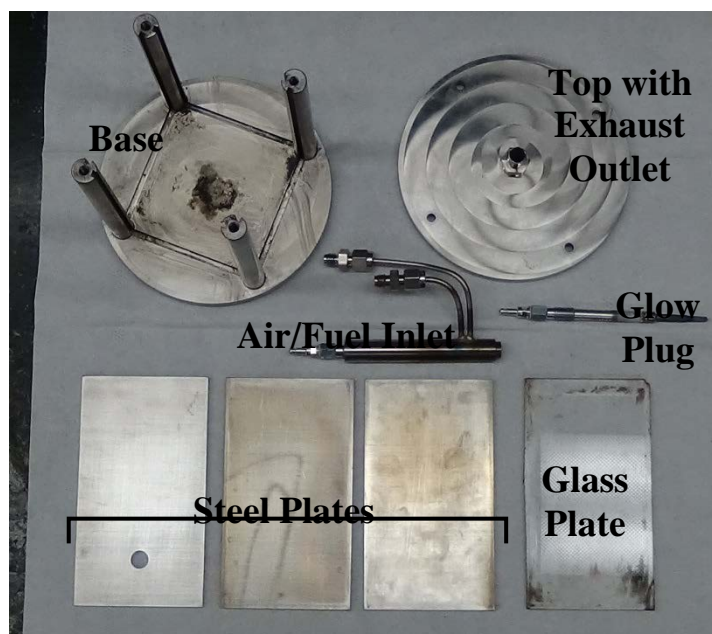


Fig. 27: Photograph of individual components of liquid-fuel combustor.

### Initial Validation Experiments

The first step was to perform a limited set of experiments to validate the combustion calculations. The exhaust outlet of the combustor was attached to an exhaust gas analyzer system comprised of two commercial analyzers (ZRE NDIR/O<sub>2</sub> multichannel analyzers; California Analytical Instruments; Orange, CA), one for measuring higher concentrations and the other for measuring lower concentrations. Concentrations of CO<sub>2</sub>, CO, SO<sub>2</sub>, NO, and CH<sub>4</sub> are measured using non-dispersive infrared (NDIR) spectroscopy, while O<sub>2</sub> concentration is measured using a paramagnetic sensor. A NO<sub>x</sub> converter unit is used to convert NO<sub>2</sub> to NO, such that the measurement of NO by the analyzer provides a measurement of total NO<sub>x</sub> in the exhaust gas. The ranges for each species that can be measured by each of the ZRE units are shown in Table 8.

Table 8: Measurement ranges of ZRE exhaust gas analyzer units for various gas species of interest. All values are volume/mole fractions.

Species	ZRE Low measurement range	ZRE High measurement range
CO	0 – 200 ppm	0 – 1000 ppm
CO <sub>2</sub>	0 – 5 vol %	N/A
SO <sub>2</sub>	0 – 500 ppm	0 – 1000 ppm
NO	0 – 200 ppm	N/A
CH <sub>4</sub>	N/A	0 – 500 ppm
O <sub>2</sub>	0 – 25 vol %	0 – 20.9 vol %

Because of the relatively high range for the SO<sub>2</sub> concentration even in the ZRE Low (low concentration detector system), accurate measurements were only expected for SO<sub>2</sub> concentrations of 10 – 20 ppm. To increase the likelihood of accurate measurement, the decision was made to evaluate fuel formulations that

were expected to produce exhaust gas with approximately 100 ppm SO<sub>2</sub>. Therefore, tests were conducted with mixtures of DTBDS (di-*t*-butyl disulfide, C<sub>8</sub>H<sub>18</sub>S<sub>2</sub>) in dodecane and tetradecane with concentrations of approximately 1250, 2500, and 5000 ppm sulfur by weight. Figure 28 shows fuel sulfur concentration based on the measured SO<sub>2</sub> concentrations compared with the known fuel sulfur concentration.

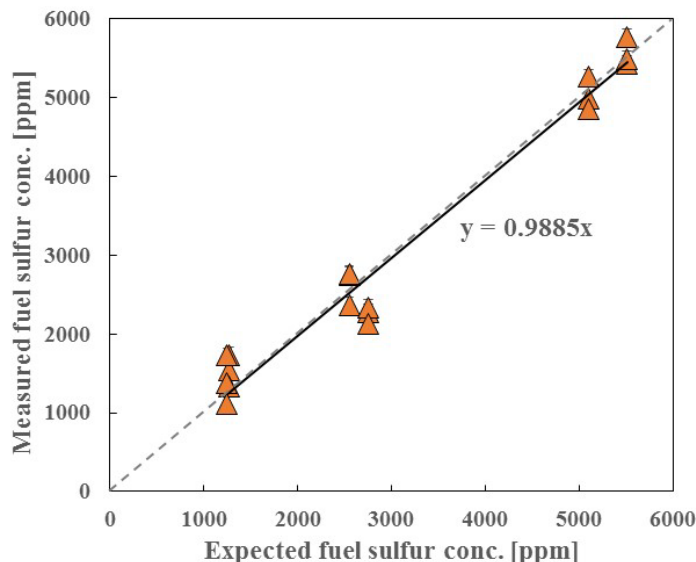


Fig. 28: Fuel sulfur concentration based on measured exhaust SO<sub>2</sub> concentration vs. known fuel sulfur concentration.

In Figure 28, the solid line represents a linear regression to the plotted data, while the dashed line illustrates the ideal case of a perfect match between known fuel sulfur concentration and the value determined from the SO<sub>2</sub> measurement. For both fuels, the measured SO<sub>2</sub> concentration related well to the known value of sulfur in the fuel. The orange triangles each represent a test conducted, three total for each fuel. The slope of the collected data was 0.99, which is very close to the ideal slope of 1.0 for a perfect match. The collected data differed from the known concentrations by only 1.15%. Because the measured values are scattered both above and below the known values, indicating random experimental variation, it seems that all of the sulfur in the fuel was being converted to SO<sub>2</sub> in the exhaust.

In a separate set of experiments, an FTIR (Fourier transform infrared) spectrometer was used to analyze the combustion exhaust. FTIR analysis provides information on chemical species present over a broad spectral range in a relatively rapid manner. A major concern, however, with FTIR measurements is the presence of water vapor, which has numerous IR absorption bands, including some that overlap or nearly overlap with a prominent SO<sub>2</sub> absorption band. The use of a dryer (thermoelectric cooler) to remove water vapor was expected to mitigate this issue. Unfortunately, the IR absorbance of SO<sub>2</sub> is weak, even for its most prominent absorption bands. Even at concentrations of hundreds of parts per million, SO<sub>2</sub> absorbance was less than 0.05 in these experiments, which was on the order of the nearby and somewhat overlapping water vapor absorbance. At the relevant SO<sub>2</sub> concentrations of < 1 ppm, there would be little to no measurable absorbance.

Based on these results, it does not appear that FTIR analysis is a viable method to measure the required low levels of SO<sub>2</sub>, particularly considering the difficulty in removing all of the water vapor. To have any chance with FTIR measurements, the instrument would need significantly better resolution to enable differentiation between SO<sub>2</sub> and water absorption lines and to improve the SO<sub>2</sub> signal itself. The

measurement also would benefit tremendously from use of an improved method of selective water removal. Regardless, the only way to achieve the sensitivity needed to measure  $< 1$  ppm  $\text{SO}_2$  with a FTIR would be to use an absorption cell with an extremely long path length. Considering the absorbance levels observed in the present experiments, a cell with path length on the order of 10 meters would likely be required.

### **Ultraviolet Fluorescence Measurements**

As seen in the previous section, validation experiments using dodecane and tetradecane with relatively high concentrations of DTBDS consistently showed near-total or total conversion of sulfur to  $\text{SO}_2$  in the combustion exhaust. These results provided the confidence to move forward with measurements using a highly sensitive  $\text{SO}_2$  analyzer that uses ultraviolet fluorescence (UVF) rather than traditional NDIR absorption. The UVF instrument is a Horiba model APSA-370 and has four  $\text{SO}_2$  measurement ranges: 0 – 0.25 ppm, 0 – 0.50 ppm, 0 – 1.25 ppm, and 0 – 2.5 ppm. The user can explicitly select one of these four ranges for a given measurement or simply set the instrument to auto-select the appropriate range.

Although initial experiments showed promise, performance of the UVF instrument rapidly deteriorated. The instrument lamp voltage decreased significantly as combustion exhaust passed through the analyzer, and this did not occur for a simple calibration mixture of  $\text{SO}_2$  in  $\text{N}_2$ . Lamp voltage is a reference measurement of the light intensity of the UV lamp inside the analyzer, and it is supposed to remain nominally constant. This signal is used by the analyzer to compensate for any loss in lamp intensity, which normally occurs slowly over a long period of time as the lamp degrades. It should not decrease rapidly during a test and then return to normal after a test, unless there is a problem. Discussions with engineers at Horiba led to the conclusion that the problem was the presence of non-negligible levels of NO and unburned hydrocarbons (UHC), which absorb UV light. These species, along with water vapor, can also condense on and degrade the glass surface of the lamp. This can lead to irreversible loss of measured lamp voltage.

In addition, the UVF instrument began to exhibit inaccurate  $\text{SO}_2$  measurements, compared to expectations. The lamp voltage issue perhaps contributed to this, since the value of lamp voltage at times was so low during operations that the analyzer considered it too low for useful measurements. In addition, NO also absorbs UV light and subsequently emits fluorescence in a spectral region that overlaps  $\text{SO}_2$  fluorescence. The APSA-370 cannot distinguish between fluorescence from NO and  $\text{SO}_2$ , thus it interprets all of it as  $\text{SO}_2$  fluorescence and gives artificially high values if NO levels are significant.

It seems that the only way to use the UVF analyzer is to dilute the combustion exhaust, which would lower the levels of unburned hydrocarbons and NO in the sample. Unfortunately, this would also dilute the  $\text{SO}_2$  levels as well, which would make it impossible to perform effective measurements in the desired range (i.e., total sulfur  $< 10$  ppm by weight in the fuel). Measurements with diluted combustion exhaust, however, could potentially be conducted for sulfur weight fractions in the fuel of perhaps 25 to 50 ppm. This is not considered sufficient for the current program, thus other methods would need to be pursued.

### **Commercial Electrochemical Sensor Measurements**

Limited experiments were performed in which exhaust from the designed combustor (see Figures 26 and 27) was directed to the Dräger sensors to quantify the  $\text{SO}_2$  concentration in the exhaust. In one case, the exhaust was not dried. In another case, the exhaust was dried using the thermoelectric cooler. In a third case, the exhaust was dried in two stages using the thermoelectric cooler followed by a water trap containing molecular sieves. Regardless of the conditions, the sensor was saturated to the maximum 100 ppm  $\text{SO}_2$  concentration, even when the fuel was *n*-dodecane with no sulfur compound added. It is unlikely that water vapor was a primary issue in these measurements, because relative humidity was  $< 10\%$  when the two-stage drying method was used. These results indicate that the cross-sensitivities to the CO, NO, and UHC in the combustion exhaust are far too strong to allow for a useful  $\text{SO}_2$  measurement.

Although these cross-sensitivities are significant with respect to this particular COTS sensor, it is at least conceivable that customized electrochemical sensors could be constructed to mitigate any interferences. Speculation on the possible makeup of such sensors, however, would rely upon specific knowledge of the proprietary makeup of the evaluated COTS sensors, which is currently unavailable.

## SUMMARY AND CONCLUSIONS

In this program, various methods to quantify sulfur in liquid fuels at weight concentrations below 10 ppm have been examined. The following observations were made:

1. Although sulfur vibrational modes exist that can, fundamentally, be detected using IR spectroscopy, these vibrational modes were unexpectedly weak when evaluated in the context of surrogate fuel samples. This lack of intensity is compounded by the low limits of detection desired for the present work. While it was initially hypothesized that multivariate data modeling could be used to extract meaningful sulfur quantifications from even thusly obfuscated data, this turned out not to be the case, a circumstance that might be at least partially attributable to the nontrivial differences in the wavenumbers at which the relevant vibrational modes were found in different sulfur-containing compounds.
2. An in-house cermet (ceramic-metallic) electrochemical sensor initially showed clear response to SO<sub>2</sub>, even for volume concentrations as low as 0.1 ppm. Qualitatively, the signal was directly and positively proportional to SO<sub>2</sub> concentration and was reasonably repeatable in multiple experiments.
3. After initial testing, the cermet sensor degraded significantly and became completely unresponsive to SO<sub>2</sub>, regardless of concentration. Attempts to revive the sensor by flash heating proved unsuccessful.
4. A small laboratory combustor that operates on small amounts of liquid fuel was developed. Initial combustion tests using an NDIR (non-dispersive infrared) exhaust gas analyzer system showed that nominally all of the sulfur a liquid fuel is converted to SO<sub>2</sub> in the exhaust, though these tests were conducted for relatively high concentrations of sulfur in the fuel.
5. Experiments using a highly sensitive UVF (ultraviolet fluorescence) SO<sub>2</sub> analyzer were unsuccessful for two reasons. First, nitric oxide (NO) and unburned hydrocarbons (UHC) in the exhaust stream cause problems for the ultraviolet (UV) lamp inside the analyzer. Second, NO exhibits fluorescence in a spectral region that overlaps SO<sub>2</sub> fluorescence, thus causing signal interference and possibly erroneous SO<sub>2</sub> measurements. These issues appear to be insurmountable with this UVF analyzer.
6. Experiments passing combustion exhaust through a Fourier transform infrared (FTIR) spectrometer showed that it was not possible to measure SO<sub>2</sub> at the low concentrations relevant to this program, corresponding to < 10 ppm sulfur in the liquid fuel. The IR absorption band of SO<sub>2</sub> is weak and partially overlaps with water absorption bands.
7. A commercial-off-the-shelf (COTS) electrochemical SO<sub>2</sub> sensor had a clear and quantifiable response to SO<sub>2</sub>, though the sensitivity and limit of detection might not be sufficient for the needs of this program. Furthermore, the sensor reading became saturated (> 100 ppm) when exposed to real combustion exhaust even without the presence of sulfur in the liquid fuel.

Based on the results, the following conclusions have been reached:

- i. Infrared (IR) spectroscopy does not have a sufficient, generalized sensitivity towards organosulfur compounds to constitute an acceptable detection method for sub-10-ppm levels of sulfur in Navy

mobility fuels. Although individual organosulfur compounds might be discernable at such concentrations in simple liquid-fuel surrogates, the use of IR spectroscopy is not deemed to be capable of quantifying total sulfur concentration in full-distillate liquid fuels.

- ii. Use of cermet sensors for measurement of SO<sub>2</sub> in combustion exhaust is promising, but would require a significant commitment from a supplier/manufacturer or research organization to identify sensor materials that do not degrade when exposed to SO<sub>2</sub> and other combustion exhaust species.
- iii. Use of commercial gas sensors using conventional optical methods for measurement of SO<sub>2</sub> in combustion exhaust does not appear to be viable. FTIR and NDIR instruments do not have the required sensitivity. UVF instruments have multiple issues, including degradation of the instrument from NO and UHC present in the combustion exhaust and signal interference from NO.
- iv. Use of commercial electrochemical sensors for measurement of SO<sub>2</sub> in combustion exhaust might hold promise, but it is not clear if these sensors have sufficient sensitivity for quantification of sulfur below 10 ppm in fuel. In addition, cross-sensitivity to other combustion exhaust species (e.g., CO, NO, UHC) would need to be addressed.

## POTENTIAL FUTURE WORK

There are several avenues of potential future work extending from this program:

1. Continued work using cermet electrochemical sensors to measure SO<sub>2</sub> in combustion exhaust. This would require commitment of resources to foster a relationship with a company (e.g., General Atomics) or a research organization (e.g., Argonne National Laboratory) that develops cermet sensors. The primary issue is identification of materials that are sensitive to SO<sub>2</sub> but do not progressively degrade.
2. Adaptation of chemiluminescence capillary GC (gas chromatography) detector technology. The primary thrust of this work would be to simplify and downsize the instrumentation for field deployment.
3. Development of a new type electrochemical sensor. One possibility that is being explored involves gold nanoparticles that interact strongly with sulfur.
4. Development of a new optical sensor to measure SO<sub>2</sub> in combustion exhaust. One possibility that is being explored is UV absorption.

## ACKNOWLEDGMENTS

The authors gratefully acknowledge the contributions of and discussions with Dr. Susan L. Rose-Pehrsson (NRL, Code 6180) and Dr. Steven G. Tuttle (NRL, Code 6185). This study was funded by Code 30, Office of Naval Research.

## REFERENCES

- [1] Kelly, L. C., and Rawson, P., 2010, "Detection and Identification of Sulfur Compounds in an Australian Jet Fuel," Technical Report No. DSTO-TN--0956, Air Vehicles Division of the Defence Science and Technology Organisation (Australia).
- [2] Link, D. D., Baltrus, J. P., and Rothenberger, K. S., 2002, "Rapid Determination of Total Sulfur in Fuels Using Gas Chromatography with Atomic Emission Detection," *J Chromatogr Sci*, **40**(9), pp. 500-504.

- [3] Agilent G2350A Atomic Emission Detector, Accessed September 2016, <https://www.agilent.com/cs/library/specifications/Public/59664141.pdf>
- [4] Amais, R. S., Nóbrega, J. A., and Donati, G. L., 2014, "Sulfur Determination in Fuels by ICP-OES and ICP-MS to Meet Increasingly Stricter Legislation Requirements," Spectroscopy (online article), Accessed September 2016, <http://www.spectroscopyonline.com/sulfur-determination-fuels-icp-oes-and-icp-ms-meet-increasingly-stricter-legislation-requirements>.
- [5] Spectro Fuel Analysis, Accessed September 2016, <http://www.spectro.com/industries/diesel-fuel-gasoline-testing-analysis>
- [6] Oxford Handheld LIBS Analyzer, Accessed September 2016, <https://www.oxford-instruments.com/OxfordInstruments/media/industrial-analysis/handheld-lib-s-analyzer/Handheld-metal-analyzer-mPulse-LIBS.pdf?width=0&height=0&ext=.pdf>
- [7] Horiba MESA-7220, Accessed September 2016, <http://www.horiba.com/scientific/products/sulfur-in-oil/ mesa-7220-details/ mesa-7220-x-ray-fluorescence-sulfur-and-chlorine-12793/>
- [8] "Standard Test Method for Sulfur in Automotive, Heating, and Jet Fuels by Monochromatic Energy Dispersive X-Ray Fluorescence Spectrometry," 2012, ASTM D7220, ASTM International.
- [9] XOS Sindie 2622, Accessed September 2016, <http://www.xos.com/sindie-benchtops/sindie-2622/family?productId=51857795153>
- [10] Oxford Lab-X3500, Accessed September 2016, [https://www.oxford-instruments.com/OxfordInstruments/media/x-ray-fluorescence/benchtup-xrf-brochures/Lab-X3500-Brochure\\_2014.pdf?width=0&height=0&ext=.pdf](https://www.oxford-instruments.com/OxfordInstruments/media/x-ray-fluorescence/benchtup-xrf-brochures/Lab-X3500-Brochure_2014.pdf?width=0&height=0&ext=.pdf)
- [11] Rigaku Sulfur Analysis, Accessed September 2016, [http://www.rigaku.com/en/applications/sulfur\\_and\\_petroleum](http://www.rigaku.com/en/applications/sulfur_and_petroleum)
- [12] Agilent Sulfur Chemiluminescence Detector, Accessed September 2016, <http://www.agilent.com/en-us/products/gas-chromatography/selective-detectors/sulfur-chemiluminescence-detector>
- [13] "Standard Test Method for Sulfur Compounds in Light Petroleum Liquids by Gas Chromatography and Sulfur Selective Detection," 2014, ASTM D5623, ASTM International.
- [14] Agilent Gas Chromatography, Accessed September 2016, <http://www.agilent.com/cs/library/datasheets/public/5991-6199EN.pdf>
- [15] Agilent SCD Image, Accessed September 2016, [http://www.agilent.com/cs/publishingimages/8355-SCD-Standalone-with-burner\\_1000x1000.jpg](http://www.agilent.com/cs/publishingimages/8355-SCD-Standalone-with-burner_1000x1000.jpg)
- [16] PAC 7090 Detector with GC, Accessed September 2016, [http://www.paclp.com/lab\\_instruments/7090\\_detector\\_with\\_gc/](http://www.paclp.com/lab_instruments/7090_detector_with_gc/)
- [17] "Standard Test Method for Determination of Sulfur Compounds in Natural Gas and Gaseous Fuels by Gas Chromatography and Chemiluminescence," 2012, ASTM D5504, ASTM International.

- [18] Dräger PAC Series, Accessed September 2016, [https://www.draeger.com/products/content/single\\_gas\\_detection\\_br\\_9046540\\_en.pdf](https://www.draeger.com/products/content/single_gas_detection_br_9046540_en.pdf)
- [19] Gainger Sulfur Dioxide Detector (Dräger), Accessed September 2016, <https://www.grainger.com/product/DRAEGER-Single-Gas-Detector-36D923?functionCode=P2IDP2PCP>
- [20] Dräger Sensor XXS, Accessed September 2016, <https://www.draeger.com/products/content/sensor-xxs-pi-9045598-en-gb.pdf>
- [21] Teledyne Model 6000/6400 Sulfur Analysis Systems, Accessed September 2016, <http://www.teledyne-ai.com/pdf/6400TS.pdf>
- [22] "Standard Test Method for Determination of Total Sulfur in Light Hydrocarbons, Spark Ignition Engine Fuel, Diesel Engine Fuel, and Engine Oil by Ultraviolet Fluorescence," 2016, ASTM D5453, ASTM International.
- [23] Teledyne 6400E, Accessed September 2016, [http://www.pasuk.com/downloads/6400E\\_SO2\\_Analyser.pdf](http://www.pasuk.com/downloads/6400E_SO2_Analyser.pdf)
- [24] Thermo Scientific SOLA II, Accessed September 2016, <https://www.thermofisher.com/order/catalog/product/SOLAXANALYZ>
- [25] California Environmental Protection Agency – Air Resources Board, 2014, "Procedure for the Determination of Sulfur in Fuels by U.V. Fluorescence," SOP No. MLD123 (Revision No. 5).
- [26] Rebinsky, D. A., Fei, D., and Zemskova, S. M., 2013, "Light based sulfur sensor and system," US Patent No. US 20130044324 A1.
- [27] CI Analytics Sulphur Analysis, Accessed September 2016, [http://www.cianalytics.com/Portals/0/Articles/eval\\_sulphur\\_measurement\\_analytical\\_techniques\\_gases\\_fuel.pdf](http://www.cianalytics.com/Portals/0/Articles/eval_sulphur_measurement_analytical_techniques_gases_fuel.pdf)
- [28] Gainger H<sub>2</sub>S Detector (Dräger), Accessed September 2016, <https://www.grainger.com/product/DRAEGER-Single-Gas-Detector-36D911?functionCode=P2IDP2PCP>
- [29] RKI Gas Detection Systems, Accessed September 2016, <http://www.rkiinstruments.com/>
- [30] Buck Scientific FPD, Accessed September 2016, <https://www.bucksci.com/products/flame-photometric-detector-fpd>
- [31] "Standard Test Method for Determination of Sulfur Compounds in Natural Gas and Gaseous Fuels by Gas Chromatography and Flame Photometric Detection," 2010, ASTM D6228, ASTM International.
- [32] Agilent FPD Plus, Accessed September 2016, [http://www.agilent.com/en-us/products/gas-chromatography/selective-detectors/flame-photometric-detector-plus-\(fpd-plus\)](http://www.agilent.com/en-us/products/gas-chromatography/selective-detectors/flame-photometric-detector-plus-(fpd-plus))
- [33] OI Analytical PFPD, Accessed September 2016, <http://www.oico.com/default.aspx?id=product&productID=57>
- [34] Haydt, D., "Determination of Hydrogen Sulfide and Total Sulfur in Natural Gas," Accessed September 2016, <http://asgmt.com/wp-content/uploads/pdf-docs/2011/1/Q01.pdf>

- [35] Hashida, T., and Wakao, K., 2016, "Control system and control method for internal combustion engine," US Patent No. US 20160349206 A1.
- [36] Daly, J. M., 2012, "Sulfur breakthrough detection assembly for use in a fuel utilization system and sulfur breakthrough detection method," US Patent No. US 20120129267 A1.
- [37] Socrates, G., 2004, *Infrared and Raman Characteristic Group Frequencies: Tables and Charts*, John Wiley & Sons, Hoboken, NJ.
- [38] de Peinder, P., Visser, T., Wagemans, R., Blomberg, J., Chaabani, H., Soulimani, F., and Weckhuysen, B. M., 2010, "Sulfur Speciation of Crude Oils by Partial Least Squares Regression Modeling of Their Infrared Spectra," *Energ Fuel*, **24**, pp. 557-562.
- [39] Muller, A. L. H., Picoloto, R. S., Mello, P. D., Ferrao, M. F., Dos Santos, M. D. P., Guimaraes, R. C. L., Muller, E. I., and Flores, E. M. M., 2012, "Total Sulfur Determination in Residues of Crude Oil Distillation Using FT-IR/ATR and Variable Selection Methods," *Spectrochim Acta A*, **89**, pp. 82-87.
- [40] Ingle Jr., J. D., and Crouch, S. R., 1988, *Spectrochemical Analysis*, Prentice Hall, Upper Saddle River, NJ.
- [41] Wagner, A. L., Amundsen, T. J., and Yelvington, P. E., 2013, "Compact, In-line Fuel Sulfur Analyzer for Improved Management of Desulfurizers," 13th Annual Meeting of American Institute of Chemical Engineers (AIChE), San Francisco, CA.
- [42] Hammond, M. H., Johnson, K. J., Rose-Pehrsson, S. L., Ziegler, J., Walker, H., Caudy, K., Gary, D., and Tillett, D., 2006, "A Novel Chemical Detector Using Cermet Sensors and Pattern Recognition Methods for Toxic Industrial Chemicals," *Sensor Actuat B-Chem*, **116**(1-2), pp. 135-144.
- [43] Kramer, K. E., Rose-Pehrsson, S. L., Hammond, M. H., Tillett, D., and Streckert, H. H., 2007, "Detection and Classification of Gaseous Sulfur Compounds by Solid Electrolyte Cyclic Voltammetry of Cermet Sensor Array," *Anal Chim Acta*, **584**(1), pp. 78-88.
- [44] Williams, B. A., Tuttle, S. G., and Fleming, J. W., 2012, "Optical Detection Approaches for Monitoring Fuel Sulfur Content," Naval Research Laboratory, NRL Letter Report NRL/2012-6180-0021. Washington, DC, February 2012.
- [45] Sigma-Aldrich FTIR Spectrum, Accessed September 2016, <http://www.sigmaaldrich.com/spectra/ftir/FTIR003854.PDF>
- [46] Cheval, N., Kampars, V., Fowkes, C., Shirtcliffe, N., and Fahmi, A., 2013, "Assembly of Poly-3-Hexylthiophene Nano-Crystallites into Low Dimensional Structures Using Indandione Derivatives," *Nanomaterials*, **3**(1), pp. 107-116.
- [47] NIST Chemistry WebBook: 3-Methylbenzothiophene, Accessed September 2016, <http://webbook.nist.gov/cgi/cbook.cgi?ID=C1455181&Mask=80>
- [48] Larrubia, M. A., Gutierrez-Alejandre, A., Ramirez, J., and Busca, G., 2002, "A FT-IR Study of the Adsorption of Indole, Carbazole, Benzothiophene, Dibenzothiophene and 4,6-Dibenzothiophene over Solid Adsorbents and Catalysts," *Appl Catal A-Gen*, **224**(1-2), pp. 167-178.

- [49] Shamsipur, M., Zare-Shahabadi, V., Hemmateenejad, B., and Akhond, M., 2006, "Ant Colony Optimisation: A Powerful Tool for Wavelength Selection," *J Chemometr*, **20**(3-4), pp. 146-157.
- [50] Silverstein, R. M., Bassler, G. C., and Morrill, T. C., 1974, *Spectrometric Identification of Organic Compounds*, John Wiley & Sons, Inc., Hoboken, NJ.
- [51] Beebe, K. R., Pell, R. J., and Seasholtz, M. B., 1998, *Chemometrics: A Practical Guide*, John Wiley & Sons, Inc., Hoboken, NJ.
- [52] Haaland, D. M., and Thomas, E. V., 1988, "Partial Least-Squares Methods for Spectral Analyses .1. Relation to Other Quantitative Calibration Methods and the Extraction of Qualitative Information," *Anal Chem*, **60**(11), pp. 1193-1202.
- [53] Kramer, K. E., Morris, R. E., Rose-Pehrsson, S. L., Cramer, J., and Johnson, K. J., 2008, "Statistical Significance Testing as a Guide to Partial Least-Squares (PLS) Modeling of Nonideal Data Sets for Fuel Property Predictions," *Energ Fuel*, **22**(1), pp. 523-534.